

Control of acute myeloid leukemia by a trifunctional NKp46-CD16a-NK cell engager targeting CD123

Received: 10 August 2022

Accepted: 23 November 2022

Published online: 12 January 2023

 Check for updates

Laurent Gauthier^{1,10}✉, Angela Virone-Oddos^{2,10}✉, Jochen Beninga³, Benjamin Rossi¹, Céline Nicolazzi², Céline Amara⁴, Audrey Blanchard-Alvarez¹, Nicolas Gourdin¹, Jacqueline Courta⁵, Alexandra Basset⁶, Magali Agnel⁷, Franceline Guillot¹, Gwendoline Grondin¹, Hélène Bonnevaux^{8,2}, Anne-Laure Bauchet⁷, Ariane Morel¹, Yannis Morel¹, Marielle Chiron² & Eric Vivier^{1,8,9}✉

CD123, the alpha chain of the IL-3 receptor, is an attractive target for acute myeloid leukemia (AML) treatment. However, cytotoxic antibodies or T cell engagers targeting CD123 had insufficient efficacy or safety in clinical trials. We show that expression of CD64, the high-affinity receptor for human IgG, on AML blasts confers resistance to anti-CD123 antibody-dependent cell cytotoxicity (ADCC) *in vitro*. We engineer a trifunctional natural killer cell engager (NKCE) that targets CD123 on AML blasts and NKp46 and CD16a on NK cells (CD123-NKCE). CD123-NKCE has potent antitumor activity against primary AML blasts regardless of CD64 expression and induces NK cell activation and cytokine secretion only in the presence of AML cells. Its antitumor activity in a mouse CD123⁺ tumor model exceeds that of the benchmark ADCC-enhanced antibody. In nonhuman primates, it had prolonged pharmacodynamic effects, depleting CD123⁺ cells for more than 10 days with no signs of toxicity and very low inflammatory cytokine induction over a large dose range. These results support clinical development of CD123-NKCE.

Acute myeloid leukemia (AML), the most common acute leukemia in adults¹, is characterized by the clonal expansion of myeloid precursors in the bone marrow (BM) and peripheral blood². There is a clear unmet medical need in AML, as up to 50% of patients relapse after initial chemotherapy³, and the prognosis for older patients remains poor¹.

Several targeted immunotherapies, such as monoclonal antibodies⁴, bispecific T (TCE) and killer cell engager molecules^{5,6} and chimeric

antigen receptor (CAR) T cells^{7,8}, are currently under clinical evaluation. They target various antigens expressed on AML blasts, with CD33 and CD123 antigens being the most frequently targeted.

CD123, the alpha chain of the interleukin-3 receptor (IL-3R α), is frequently expressed at high levels in AML^{9,10}, mostly on leukemic stem or progenitor cells¹¹, associated with a poor prognosis. Cytotoxic antibodies targeting CD123 displayed limited antileukemic

¹Innate Pharma, Marseille, France. ²Sanofi Immuno-Oncology Research, Vitry sur-Seine, France. ³Sanofi Large Molecules Research, Frankfurt, Germany.

⁴Sanofi Drug Metabolism and Pharmacokinetics, Chilly Mazarin, France. ⁵Sanofi TMED Biomarkers and Clinical Bioanalysis, Chilly Mazarin, France.

⁶Sanofi Preclinical Safety, Chilly Mazarin, France. ⁷Sanofi Global Project Management, Vitry sur-Seine, France. ⁸Aix-Marseille University, Centre of National Scientific Research (CNRS), National Institute of Health and Medical Research (INSERM), Centre of Immunology at Marseille-Luminy (CIML), Marseille, France.

⁹APHM, Marseille-Immuno-pole, University Hospital of Timone, Marseille, France. ¹⁰These authors contributed equally: Laurent Gauthier,

Angela Virone-Oddos. ✉e-mail: laurent.gauthier@innate-pharma.fr; Angela.Virone-Oddos@sanofi.com; eric.vivier@innate-pharma.fr

activity in several clinical trials¹², even when specifically engineered to increase antibody-dependent cell cytotoxicity (ADCC)¹³. By contrast, TCE molecules and CAR-T cells have some clinical efficacy^{5,14}, but are also highly toxic, confirming the need for alternative targeted approaches.

NK cell-based therapies may provide new treatment perspectives and a safer alternative for targeting AML cells in this context^{15–18}, without the complications frequently associated with T cell therapies, such as cytokine release syndrome or neurotoxicity¹⁹. NK cells are innate lymphoid cells that can recognize and kill virus-infected cells or cancer cells^{20–22}. Several activating receptors can be targeted to induce NK cell-mediated antitumor immunity²³, including CD16a (FcγRIIIa), NKG2D, and the natural cytotoxicity receptors (NCRs) NKp30 and NKp46 (refs. 24–26). Because the full activation of NK cells requires the coengagement of different activating receptors^{27,28}, we have developed an antibody-based NK cell engager (NKCE) technology for the generation of trifunctional molecules (NKp46-CD16a-NKCEs) targeting antigens expressed on cancer cells and coengaging NKp46 and CD16a on NK cells^{29,30}. NKp46 (NCR1, CD335) is an activating cell-surface glycoprotein highly conserved in mammals²⁵. NKp46 is expressed on all NK cells³¹, ILC1 and very small T cell and ILC3 subsets³². NKp46 signaling is mediated by association with CD3ζ and FcRγ, which trigger NK cell activation, cytotoxicity and cytokine release³³. The development of AML blasts in bone marrow affects normal hematopoiesis and the development of immune cells, including NK cells³⁴. NK cells from patients with AML often express low levels of NKp46 at diagnosis³⁵, but induction chemotherapies can restore NK cell function and normal NKp46 expression³⁶, and high levels of NKp46 at the cell surface correlate with better outcomes in allogeneic stem cell transplantation in patients with AML³⁷.

The genetic heterogeneity of AML can also translate into complex expression profiles for various cell-surface markers³⁸ including the Fc-gamma receptors (FcγRs) CD16, CD32 and CD64 (ref. 39). CD64 (FcγRI) is a high-affinity receptor for human IgG expressed on healthy monocytes and macrophages⁴⁰; it is expressed on AML blasts in about one-third of patients^{38,39}.

We report here the development of a trifunctional NKCE molecule (CD123-NKCE) targeting CD123 on AML cells. We observed that the expression of CD64 on AML cells from patients inhibited the ADCC induced by antibodies targeting CD123 in vitro and ex vivo, but had no effect on CD123-NKCE, which displayed potent antitumor activity against primary malignant AML blasts and cell lines regardless of CD64 expression.

Results

CD64 expression on AML cells inhibits anti-CD123 antibody ADCC

We investigated whether NKp46-based NKCE technology could provide more effective antitumor activity than regular IgG antibodies for AML treatment. We generated a NKCE molecule targeting CD123, evaluated the ex vivo antitumor activity of this molecule, and compared it with an antibody derived from clone 7G3 (CD123-IgG1⁺)⁴¹ engineered for enhanced ADCC⁴².

The anti-CD123 antibody-mediated killing of primary blasts from patients with AML (AML no. 1 to AML no. 7) was evaluated ex vivo with NK cells from healthy donors as effectors (Fig. 1a). The anti-CD123 antibody (CD123-IgG1⁺) mediated the killing of blasts from about half the samples from patients (AML no. 1 to 3; Fig. 1a) but was barely active against blasts from the other half of samples (AML no. 4 to 7; Fig. 1a), therefore separating samples into two groups: CD123-IgG1⁺-responders and CD123-IgG1⁺-nonresponders. The difference between these two groups cannot be accounted for by simple differences in the expression of CD123, as samples from patients with similar CD123 levels were distributed between the two groups (Fig. 1b). One notable difference between the two groups was the absence of FcγR expression

on the AML blasts of CD123-IgG1⁺-responders and its presence in CD123-IgG1⁺-nonresponders, whose cells expressed CD32 (a and/or b isoforms) and/or CD64 (Fig. 1b). We therefore hypothesized that the expression of the FcγRs CD32 and/or CD64 on malignant AML cells might interfere with ADCC, by sequestering the antibody Fc in cis at the surface of CD123⁺FcγR⁺ target cells. We tested this hypothesis by evaluating the killing activity of CD123-IgG1⁺ further with two standard AML cell lines, MOLM-13 and THP-1, which express CD123 at similar levels but differ in their expression of FcγRs (Fig. 1c). MOLM-13 cells had much lower levels of CD64 and CD32 than THP-1 cells. CD123-IgG1⁺ was active against MOLM-13 cells (CD32^{low}, CD64^{low}) and completely inactive against THP-1 cells (CD32⁺; CD64⁺) cells. For clarification of the potential respective roles of CD32 and CD64 in resistance to CD123-IgG1⁺ killing, we selectively knocked down the expression of CD32a, CD32b and CD64 in THP-1 cells. We then evaluated CD123-IgG1⁺ killing activity on THP-1 subclones expressing CD32 only, CD64 only, or both CD32 and CD64 (Fig. 1c). We found that CD64 played a dominant role in resistance to ADCC, as CD123-IgG1⁺ killing activity was restored only in the absence of CD64 expression. These results support the hypothesis that the cis capture of antibody Fc by high-affinity FcγR CD64 at the surface of the target cell interfered with ADCC, probably by competing with trans binding to CD16a on NK cells.

CD123-NKCE overcome CD64-mediated inhibition of AML killing

Unlike cytotoxic antibodies, NKCE molecules engaging NKp46 can promote NK cell cytotoxicity in a CD16a-independent manner²⁹. We therefore explored whether NKCE molecules engaging only NKp46 or coengaging both NKp46 and CD16a, could induce the NK cell-mediated killing of CD64-expressing AML target cells.

NK cell engager molecules targeting CD123 on AML cells and engaging NKp46 (NKp46-Fc null-CD123), or coengaging NKp46 and CD16a (NKp46-Fc-CD123: CD123-NKCE) on NK cells (Fig. 2a and Supplementary Figs. 1 and 2) were generated. NKp46-Fc null-CD123 was built with a silenced version of human IgG1-Fc (Fc null) mutated at position 297 (EU-numbering). The Fc of NKp46/CD16a coengager molecule (CD123-NKCE) was not modified and binds all FcγRs with regular affinity (Extended Data Table 1). Anti-NKp46 and anti-CD123 antibody moieties bind to human NKp46 and CD123 with monovalent dissociation constant (K_D) of 16.6 ± 1.1 and 0.40 ± 0.02 nM, respectively (Extended Data Table 1).

As already described for other target antigens and cancers²⁹, a bifunctional NKp46-NKCE targeting CD123 (NKp46-Fc null-CD123) had strong antitumor effects against the MOLM-13 AML cell line in vitro (Fig. 2b). The coengagement of NKp46 and CD16a with trifunctional NKCEs potentiated NK cell activation (Fig. 2b), CD123-NKCE demonstrating potent killing activity (geometric mean half-maximum effective concentration (EC_{50}) of 4.2 (95% confidence interval (CI): 2.9, 6.3) pM, and mean observed maximum specific lysis of $71 \pm 5\%$) and good consistency between NK cells from healthy donors (Fig. 2c). Moreover, we confirmed that CD123-NKCE activated NK cells and promoted the expression of the activation marker CD69, degranulation marker CD107a, TNFα, IFN-γ and MIP-1β effector cytokines/chemokines in a dose-dependent manner, exclusively in the presence of target cells expressing CD123 (Fig. 2d).

Unlike anti-CD123 antibody, both bifunctional and trifunctional NKp46 engager molecules mediated strong killing of CD64-positive THP-1 cells (Fig. 3a). We observed that trifunctional CD123-NKCE was equally potent against the parental THP-1 cells, THP-1 subclones and MOLM-13 cells, regardless of CD64 expression status on target cells (Figs. 2c and 3a).

In addition, we also compared the activity of NKp46-Fc null-CD123 and CD123-NKCE on CD64-negative and CD64-positive primary sample AML no. 2 and AML no. 4 (Fig. 3b). We observed that bifunctional

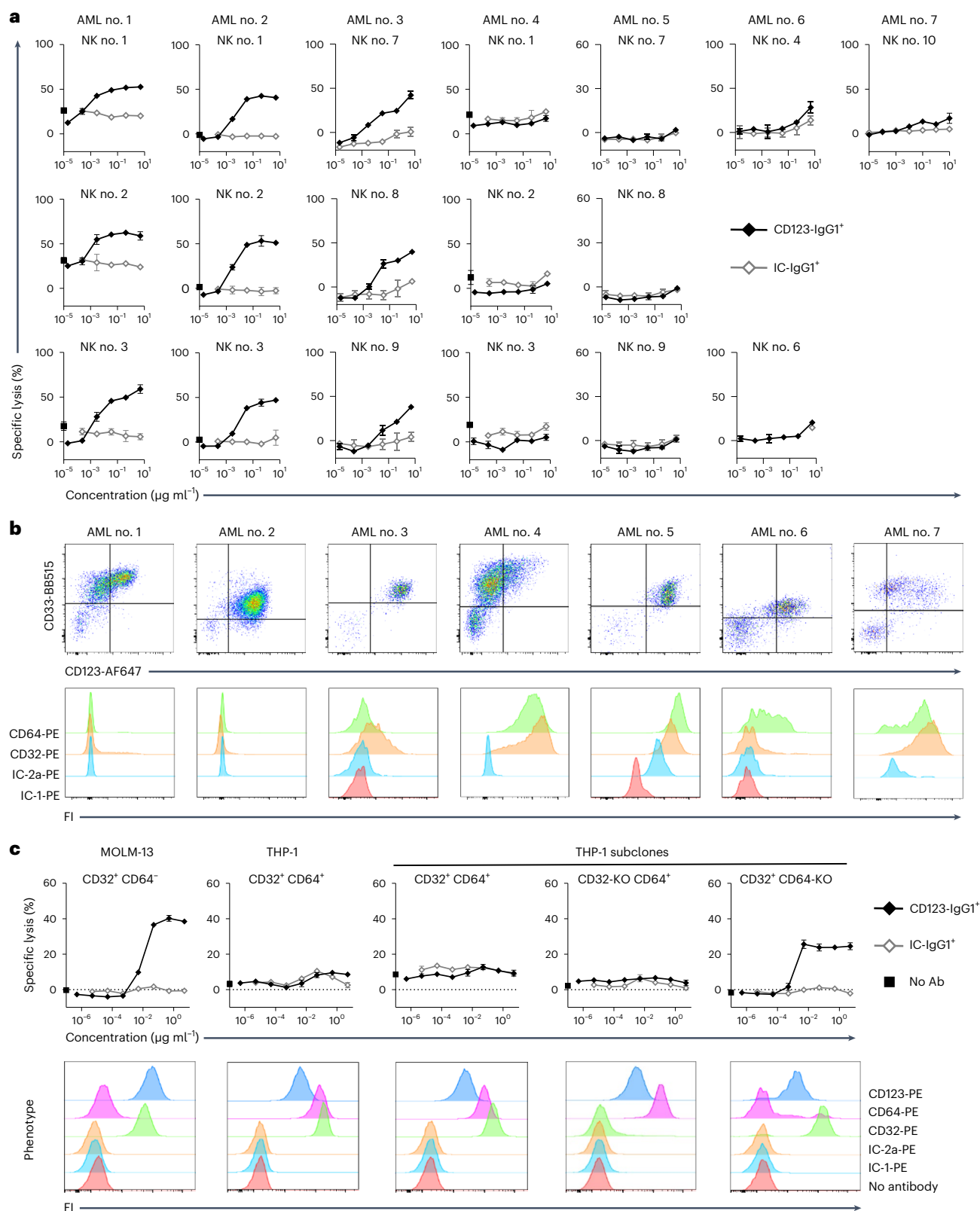


Fig. 1 | The expression of high-affinity Fc γ R CD64 on AML cells inhibits the ADCC activity of the anti-CD123 antibody in vitro. **a**, Cytotoxicity of the anti-CD123 antibody (CD123-IgG1⁺) against AML blasts from patients. Malignant cells from seven patients with AML were used as targets and purified NK cells from ten healthy donors were used as effectors. Results are shown for all healthy donor NK cells tested. **b**, Phenotype of the malignant AML cells from patients used in **a** showing the expression of CD33, CD123, CD32a/b and CD64. FI, fluorescence intensity. **c**, Upper panels show the cytotoxicity of anti-CD123

antibody (CD123-IgG1⁺) against AML cell lines with and without expression of CD32 and CD64. MOLM-13 (CD32^{low}CD64⁻) and THP-1 (CD32⁺CD64⁺) cells and THP-1 subclones with inactivated CD32 (CD32-KO CD64⁺) or CD64 (CD32⁺CD64-KO) expression were used as the target cells, with purified resting NK cells from healthy donors as effectors ($n = 3$). Data of **a** and **c** are presented as mean values \pm s.d. Lower panels show the phenotype of the AML cell lines expressing CD123, CD32 and CD64. Ab, antibody.

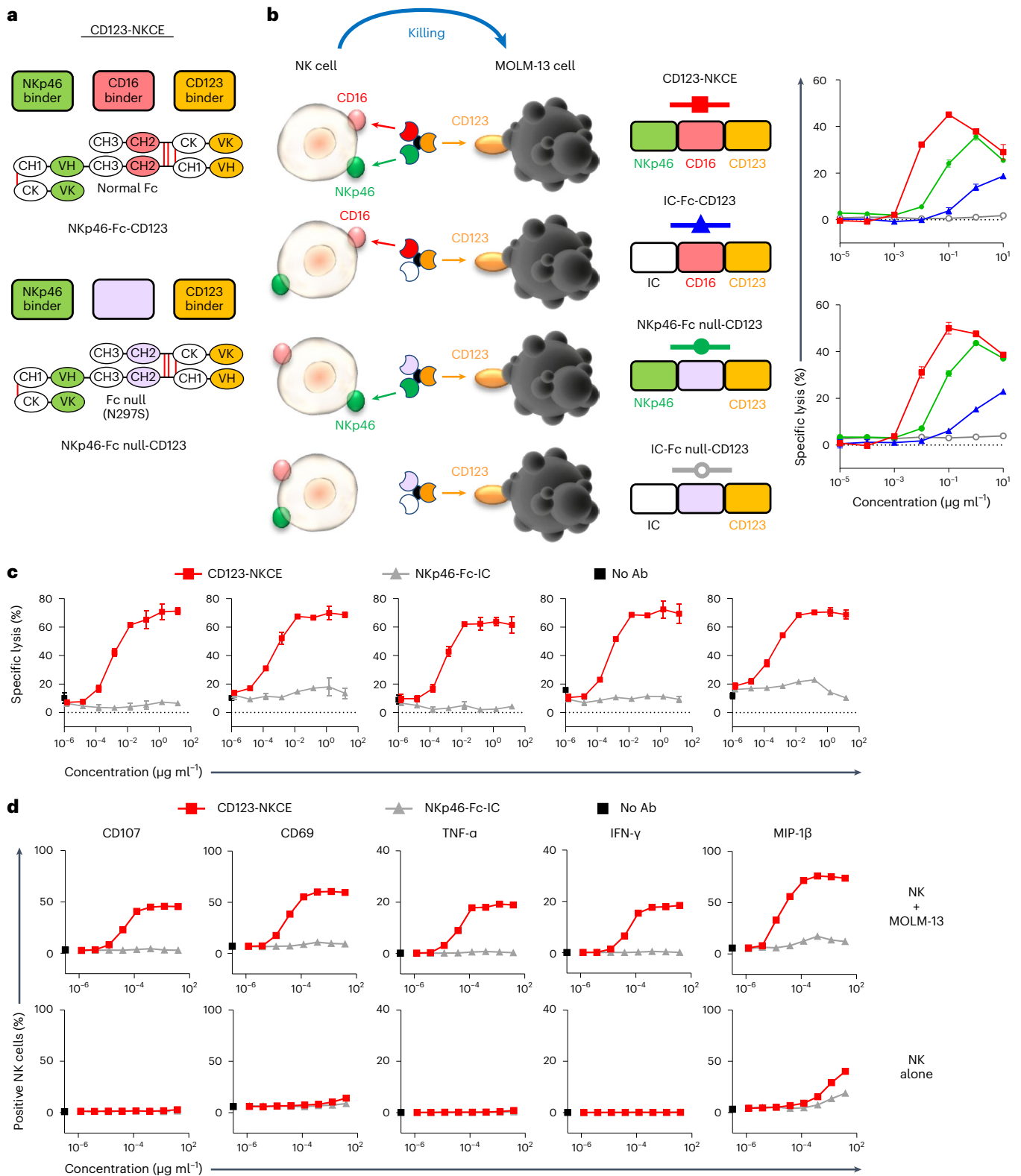


Fig. 2 | CD123-NKCE displays strong cytotoxic activity against AML cells, strong activation of NK cells and no off-target effects. **a**, Diagrams showing the molecular organization of the NKCE molecules. The top shows the CD123-NKCE trifunctional molecule built with an unmodified human IgG1-Fc (red), targeting CD123 (orange) and coengaging NKp46 (green) and CD16a on NK cells. The bottom shows the bifunctional NKCE containing a human IgG1-Fc silenced for binding to all Fc γ Rs (Fc null; purple). **b**, Comparison of the cytotoxicities of NKCEs targeting CD123 and engaging CD16a only (IC-Fc-CD123), NKp46 only (NKp46-Fc null-CD123) or coengaging NKp46 and CD16a (NKp46-Fc-CD123);

CD123-NKCE). MOLM-13 cells were used as the targets and purified resting NK cells as effectors. Results for two healthy donors are shown ($n = 3$). Data are presented as mean values \pm s.d. **c**, Cytotoxicity of CD123-NKCE against the AML cell line MOLM-13. Results for five healthy donors are shown. Data are presented as mean values \pm s.d. **d**, Evaluation, by flow cytometry, of CD107, CD69, TNF- α , IFN- γ and MIP-1 β expression by NK cells treated with CD123-NKCE. NK cells alone are compared with NK cells cocultured with MOLM-13 cells. Results for one representative donor are shown ($n = 3$).

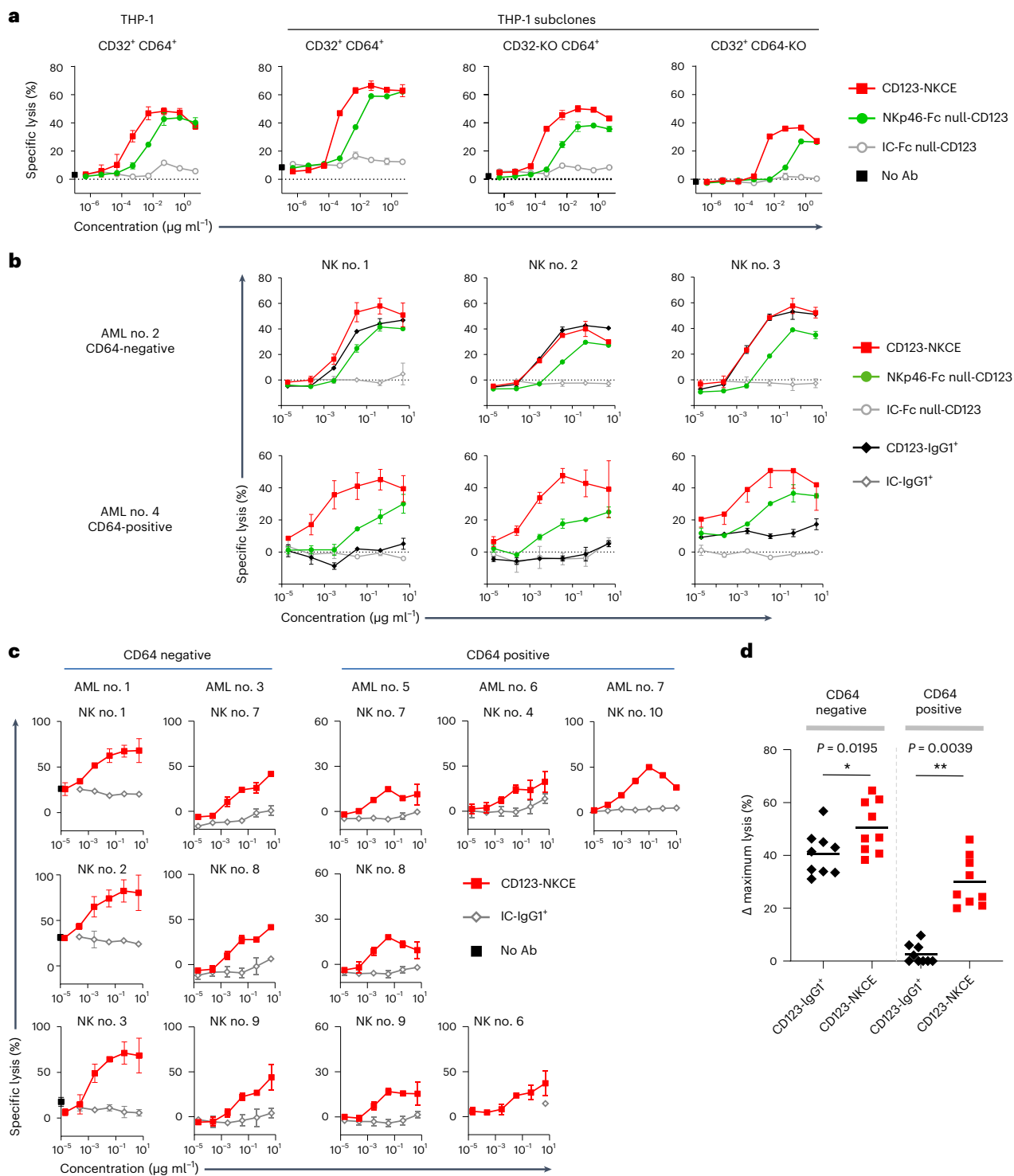


Fig. 3 | CD123-NKCE displays strong cytotoxic activity against AML cells that is not affected by expression of CD64. **a**, Comparison of the cytotoxicities of NKCE molecules engaging only Nkp46 (Nkp46-Fc null-CD123) or coengaging Nkp46 and CD16 (CD123-NKCE) against AML cell lines with and without CD32 and CD64 expression. THP-1 (CD32⁺ CD64⁺) cells and THP-1 subclones with inactivated CD32 (CD32-KO CD64⁺) or CD64 (CD32⁺ CD64-KO) expression were used as the targets, and purified resting NK cells from healthy donors were used as effectors. The data of one representative experiment among three are shown. **b**, Comparison of the cytotoxicities of CD123-IgG1⁺ (black lozenge), Nkp46-Fc null-CD123-NKCE (green circle) and CD123-NKCE (red square) against primary AML blasts expressing or not CD64. Primary AML blasts CD64-negative (AML no. 2) and CD64-positive (AML no. 4) were used as the targets and purified resting NK cells as effectors. The data for three healthy donor NK cells are shown.

c, Cytotoxicity of CD123-NKCE against blasts from patients with AML. five blasts from patients with AML (AML nos. 1, 3, 5, 6 and 7) were used as targets, and purified NK cells from healthy donors ($n = 9$) were used as effectors. Results are shown for all the healthy NK cell donors tested. Data of **a** and **c** are presented as mean values \pm s.d. **d**, Maximum cytotoxic activities of CD123-IgG1⁺ and CD123-NKCE molecules against blasts from patients with AML. Blast cells from seven patients with AML were used as targets and purified NK cells from ten healthy donors were used as effectors. Delta (Δ) maximum lysis, defined as percentage maximum lysis of the compound minus percentage background lysis of the isotype control molecule (IC-IgG1⁺ or IC-NKCE), were monitored from the dose response of each compound, and plotted separately for all couples of primary CD64-positive and CD64-negative AML sample/NK donor. (* $P \leq 0.05$; ** $P \leq 0.005$; two-sided Wilcoxon matched-pairs signed rank test).

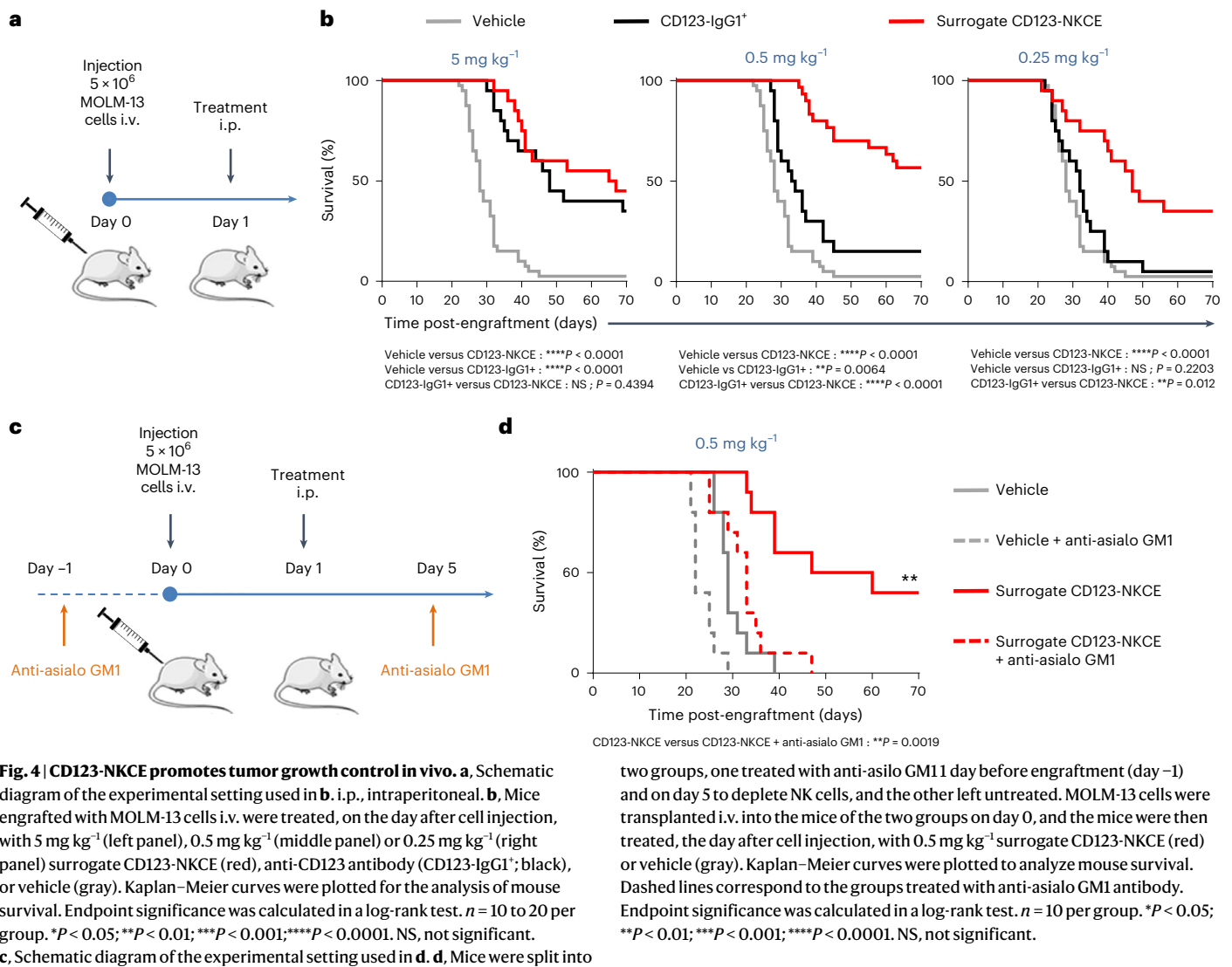


Fig. 4 | CD123-NKCE promotes tumor growth control in vivo. **a**, Schematic diagram of the experimental setting used in **b**. **i.p.**, intraperitoneal. **b**, Mice engrafted with MOLM-13 cells i.v. were treated, on the day after cell injection, with 5 mg kg⁻¹ (left panel), 0.5 mg kg⁻¹ (middle panel) or 0.25 mg kg⁻¹ (right panel) surrogate CD123-NKCE (red), anti-CD123 antibody (CD123-IgG1⁺; black), or vehicle (gray). Kaplan–Meier curves were plotted for the analysis of mouse survival. Endpoint significance was calculated in a log-rank test. $n = 10$ to 20 per group. * $P < 0.05$; ** $P < 0.01$; *** $P < 0.001$; **** $P < 0.0001$. NS, not significant. **c**, Schematic diagram of the experimental setting used in **d**. **d**, Mice were split into

two groups, one treated with anti-asialo GM11 day before engraftment (day -1) and on day 5 to deplete NK cells, and the other left untreated. MOLM-13 cells were transplanted i.v. into the mice of the two groups on day 0, and the mice were then treated, the day after cell injection, with 0.5 mg kg⁻¹ surrogate CD123-NKCE (red) or vehicle (gray). Kaplan–Meier curves were plotted to analyze mouse survival. Dashed lines correspond to the groups treated with anti-asialo GM1 antibody. Endpoint significance was calculated in a log-rank test. $n = 10$ per group. * $P < 0.05$; ** $P < 0.01$; *** $P < 0.001$; **** $P < 0.0001$. NS, not significant.

and trifunctional NKCE were active on both CD64-negative and CD64-positive AML samples, and that CD123-NKCE was consistently more potent than the bifunctional molecule.

Moreover, trifunctional NKCE molecules also displayed killing activity against all primary AML cells (Fig. 3c), promoting significant antitumor activity in CD64-positive samples from patients with AML (AML nos. 4–7) against which the regular anti-CD123 cytotoxic antibody was completely inactive. The maximum cytotoxic activities (Δ maximum lysis) of CD123-IgG1⁺ and CD123-NKCE were compared on both CD64-positive and CD64-negative primary AML groups (Fig. 3d). We observed that CD123-NKCE molecule was significantly superior to CD123-IgG1⁺ on CD64-negative samples on which the IgG1 was nevertheless active (* $P = 0.0195$), and highly superior to CD123-IgG1⁺ on CD64-positive samples on which the latter was inactive (** $P = 0.0039$).

The superiority of CD123-NKCE was confirmed on a large panels of AML cell lines (Extended Data Fig. 1a–c) coexpressing or not CD64 at the cell surface and expressing CD123 at various cell-surface densities with antibody binding capacity ranging from 580 to more than 10,000 antibody sites per cell (Extended Data Fig. 1a).

For all the CD64-negative or low cell lines (that is, KG-1a, M-07e, EOL-1, Kasumi-1, F36-P, Kasumi-6, MOLM-13 and GDM-1) the Δ maximum killing activity was comparable between CD123-IgG1⁺ and NKp46-Fc

null-CD123 molecule (Extended Data Fig. 1b,c). NKCE molecule was consistently active on all CD64-positive AML cell lines (that is NB-4, OCI-AML2, MV4-11, OCI-AML3, THP-1 and SKM-1) whatever the CD64 density of expression, with maximum killing activity globally comparable to those observed for CD64-negative or low cell lines. On the contrary, CD123-IgG1⁺ was completely inactive on OCI-AML2, OCI-AML3, THP-1 and SKM-1 CD64-positive cell lines, and showed limited activity on NB-4 and MV4-11 compared to the NKCE that was significantly highly superior to CD123-IgG1⁺ (Extended Data Fig. 1c, $P < 0.0001$), confirming with AML cell lines the results observed on primary AML samples.

An autologous NK cell activation assay performed with additional samples from patients with AML, two CD64-positive (AML nos. 8 and 9) and one CD64-negative (AML no. 10) (Extended Data Fig. 2a,b), further confirmed that, unlike CD123-IgG1⁺, which was active only against the CD64-negative sample (AML no. 10), CD123-NKCE mediated the autologous activation of NK cells from the three patients against their own blasts regardless of CD64 expression (Extended Data Fig. 2b).

CD123-NKCE controls AML tumor growth in vivo

We then assessed the in vivo efficacy of trifunctional CD123-NKCE in a xenogeneic disseminated AML tumor model induced by the intravenous (i.v.) injection of MOLM-13 tumor cells. We used a surrogate trifunctional molecule targeting the previously validated 29A1.4

epitope of mouse Nkp46 (refs. 29, 43) and human CD123 (Fig. 4a,b). The surrogate CD123-NKCE was more effective than the comparator anti-CD123 antibody over a range of doses, with 40 and 60% of mice rescued from death at doses of 0.25 and 0.5 mg antibody per kilogram body weight, versus no mice rescued at these doses in the CD123-IgG1⁺-treated groups. CD123-NKCE was also more effective than CD123-IgG1⁺ at the highest dose (5 mg kg⁻¹), with 45% of mice rescued and a 135% increase in lifespan in the NKCE group, versus 35% of mice rescued and an increase in lifespan of 70% in the antibody group (Fig. 4b). The depletion of mouse NK cells by treatment with anti-asialoGMI antibodies totally abolished CD123-NKCE efficacy in that model (Fig. 4c,d), confirming the major role of NK cells in the anti-tumor activity of trifunctional NKCE molecules in vivo.

CD123-NKCE is active and safe ex vivo and in nonhuman primates

Potent cytotoxicity may be associated with toxicity in patients. We therefore measured cytokine release from human peripheral blood mononuclear cells (PBMCs) induced by CD123-NKCE in vitro, comparing the results with those of a CD3 T cell engager antibody tool (CD123-TCE) targeting the same antigen⁵. PBMCs of healthy donors (*n* = 10) were cultured for 20 h in the presence of CD123-NKCE or CD123-TCE, and the secretion of IL-6, IL-1β, TNF-α and IFN-γ was quantified (Fig. 5a).

CD123-NKCE induced much lower levels of cytokine release than CD123-TCE, even at concentrations that were 42 times higher (Fig. 5a).

CD123 is expressed on a subset of circulating basophils and plasmacytoid dendritic cells (pDC). Given the low abundance of pDCs among human PBMCs, we focused on basophils to monitor the depletion of CD123⁺ cells by flow cytometry in the same assay (Fig. 5b,c). The treatment of PBMCs with CD123-NKCE promoted a dose-dependent partial depletion of CD123⁺ basophils with a median maximum depletion of 37% (31; 50), and a median EC₅₀ value of 38 pM (95% CI (13; 408)), calculated with six of ten donor samples (Fig. 5b,c). Thus, effective NK cell activation and recruitment by CD123-NKCE were associated with a pharmacodynamics effect of CD123⁺ cell depletion in human PBMCs, but without marked proinflammatory cytokine release at up to 10 μg ml⁻¹ dose (68 nM), suggesting that NKCEs have a better benefit/risk profile than TCEs for the treatment of AML.

We further performed dedicated pharmacokinetic, pharmacodynamics and toxicology studies in nonhuman primates (NHPs). Cynomolgus monkeys were selected as a relevant species for these studies on the basis of their tissue distributions of Nkp46 and CD123, which are similar to those in humans^{43,44}, and because the CD123-NKCE molecule binds to cynomolgus antigens and Fc receptors with affinities similar to those of human (Extended Data Table 1). In addition, a regulatory cross-reactivity study⁴⁵ performed by immunohistochemistry with the CD123-NKCE molecule on panels of human and cynomolgus normal tissues, confirmed similar staining distribution in endothelial cells of

vessels and in mononuclear cells in many organs on both species, with tissue localization similar to those previously reported for Nkp46 and CD123 antigens^{46,47}.

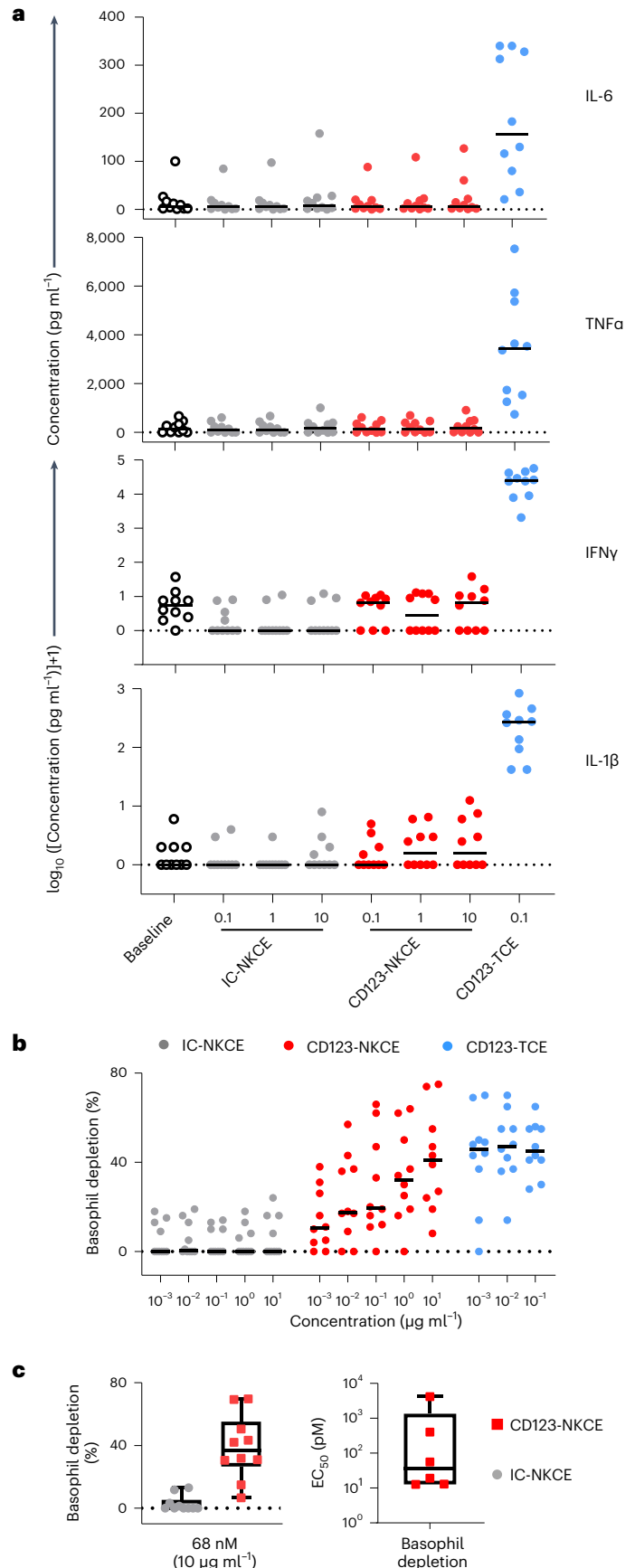


Fig. 5 | CD123-NKCE mediates pharmacodynamics effects in human PBMCs with negligible cytokine release as compared to CD123-TCE. a, IL-1β, TNF-α, IFN-γ and IL-6 cytokine release in vitro by PBMCs from healthy donors (*n* = 10) following the administration of CD123-NKCE (dose range 0.1 to 10 μg ml⁻¹), control NKCE, or a bispecific T cell engager tool targeting the same antigen (CD123-TCE, 0.1 μg ml⁻¹). Individual (dot) and median (bar) values are shown. **b**, CD123-positive basophil depletion activity in healthy donor PBMCs (*n* = 10) following the administration of CD123-NKCE (dose range 0.001 to 10 μg ml⁻¹), control NKCE (IC-NKCE) or CD123-TCE (dose range 0.001 to 0.1 μg ml⁻¹). **c**, Left panel shows a boxplot, with whiskers showing minimal and maximal value and upper and lower quartile box limits, of CD123-NKCE maximum depletion activity of the ten donors at the highest dose tested (10 μg ml⁻¹, 68 nM). Right panel shows a boxplot, with whiskers showing minimal and maximal value and upper and lower quartile box limits, of EC₅₀s for CD123-positive basophil depletion calculated from CD123-NKCE dose responses for six healthy donors among ten.

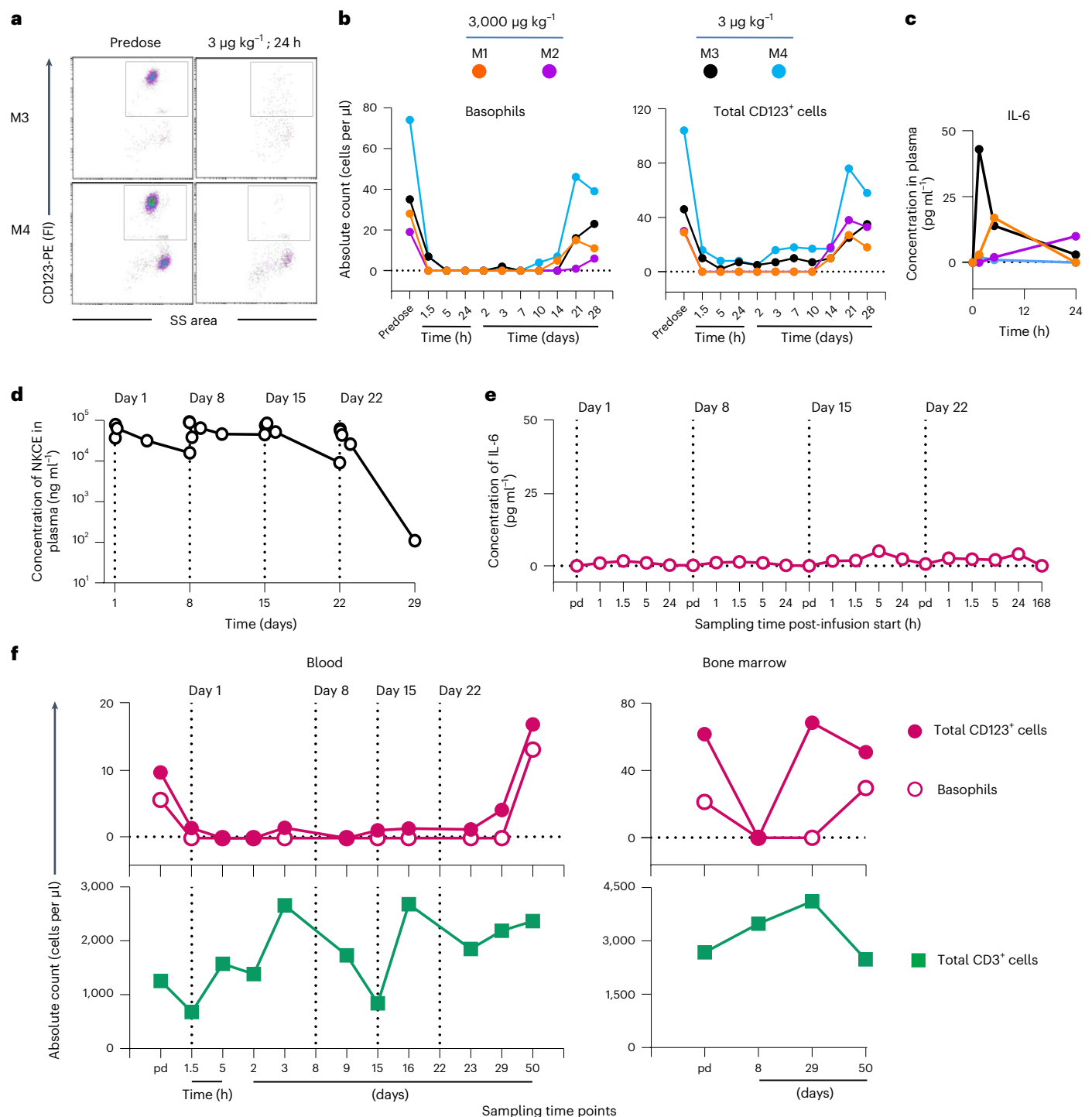


Fig. 6 | CD123-NKCE is safe and induces pharmacodynamic effects through the sustained depletion of CD123-positive cells in NHPs. a, Depletion of CD123-positive basophils (gated population) from the blood of monkeys M3 and M4 treated at the low dose of $3 \mu\text{g kg}^{-1}$ was analyzed by flow cytometry before dosing (predose, pd) and 24 h after the start of the infusion. **b**, Numbers of circulating CD123-positive basophils (left panel) and total CD123-positive leukocytes (right panel) at time of study in monkeys M1 (orange) and M2 (purple) treated with 3 mg kg^{-1} , and monkeys M3 (black) and M4 (blue) treated with $3 \mu\text{g kg}^{-1}$. **c**, IL-6 concentration in plasma of monkeys M1, M2, M3 and M4 are shown before dosing (0), and 1.5, 5 and 24 h after the start of the treatment. **d**, Toxicokinetics of the CD123-NKCE molecule in male monkey M5 weekly treated at a dose of 3 mg kg^{-1} per administration for 4 weeks (on days 1, 8, 15 and 22). Plasma CD123-NKCE concentrations were determined before dosing (predose) and 1, 1.5, 5, 24 and

72 h after the start of the 1-h infusion on days 1, 8, 15 and before dosing and 1, 1.5, 5, 24 and 168 h after the start of the last infusion on day 22. Values below the lower limit of quantification (LLOQ, 0.25 ng ml^{-1}) are not reported on the graphs. Infusion days are indicated by vertical dotted lines. **e**, Plasma IL-6 concentrations of monkey M5 were monitored before dosing and 1, 1.5, 5 and 24 h after the start of the 1 h infusion on days 1, 8, 15 and before dosing and 1, 1.5, 5, 24 and 168 h after the start of the last fourth infusion on day 22. **f**, Upper panels show the number of circulating CD123-positive basophils (open symbols) and total CD123-positive leukocytes (closed symbols) in blood (left panel) or bone marrow (right panel), by timepoint in the study, for monkey M5, treated at a dose of 3 mg kg^{-1} per week. Lower panels show the number of circulating CD3-positive T cells (green square) in blood (left panel) or bone marrow (right panel).

We evaluated the pharmacokinetic/pharmacodynamics of CD123-NKCE administered by a single 1-hour i.v. infusion of a high (3 mg kg^{-1}) or low (3 and $0.5 \text{ } \mu\text{g kg}^{-1}$) doses in male cynomolgus monkeys (two animals each for the 3 mg kg^{-1} and $3 \text{ } \mu\text{g kg}^{-1}$ doses and one animal for the $0.5 \text{ } \mu\text{g kg}^{-1}$ dose). Treatment with CD123-NKCE promoted a sustained and complete depletion of CD123⁺ cells in the blood of all monkeys, for more than 10 days, at both the 3 mg kg^{-1} and $3 \text{ } \mu\text{g kg}^{-1}$ doses (Fig. 6a,b), with only very small amounts ($<50 \text{ pg ml}^{-1}$) of the pro-inflammatory cytokines IL-6 and IL-10 released (Fig. 6c and Extended Data Fig. 3a) without any associated clinical signs.

A transient and partial depletion of CD123⁺ cells was observed in the monkey treated at the lowest dose ($0.5 \text{ } \mu\text{g kg}^{-1}$, Extended Data Fig. 3b), but $3 \text{ } \mu\text{g kg}^{-1}$ was considered to be the lowest effective dose in this species. The pharmacokinetic profiles of the two monkeys treated at 3 mg kg^{-1} demonstrated a sharp drop in plasma concentrations from 7 to 10 days after dosing due to antidrug antibody (ADA) response (Extended Data Fig. 3c,d).

We further investigated the preclinical toxicology profile of CD123-NKCE, through an exploratory repeat-dose toxicity study in which eight monkeys (two per sex per dose) were treated weekly, for 4 weeks, at 3 or 0.1 mg kg^{-1} per administration. Exposure to CD123-NKCE lasted for at least 2 weeks at both doses (Extended Data Table 2), with the presence of ADA detected from the third administration (Day 15) in all monkeys except M5 (Fig. 6d and Extended Data Table 3). Transient minimal increases in IL-6 concentration were observed after each weekly administration, for both doses (Extended Data Table 4; maximum levels of 23 and 160 pg ml^{-1} for 0.1 and 3 mg kg^{-1} per administration, respectively). In particular, no substantial IL-6 release was observed in monkey M5 that did not exhibit an ADA response (Fig. 6e), and was exposed to CD123-NKCE throughout the study (Fig. 6d) with strong specific pharmacodynamics effects of CD123⁺ cell depletion in bone marrow and in blood up to 7 days after the last administration (Fig. 6f). In all the other animals, a sustained depletion of CD123-expressing cells was observed in the blood 1.5 h after the first administration and at least up to 24 h after the third administration. Moreover, all monkeys presented a complete depletion of CD123-positive cells from the bone marrow on day 9 (24 h after the second administration), for both doses (Extended Data Table 5), with a restoration of CD123-positive populations 1 week after the last administration.

No clinical signs, changes in body weight or body temperature and no effects on electrocardiogram potentially attributable to treatment with CD123-NKCE were observed, whatever the dose. Also, no compound-related adverse effects on hematological, coagulation, clinical chemistry or urinary parameters were observed. Overall, these results thus constitute proof-of-principle for the efficacy of CD123-NKCE in vivo, with no signs of toxicity.

Discussion

There is a clear unmet medical need for patients with AML who relapse after chemotherapy. The development of targeted therapies, such as monoclonal antibodies mediating ADCC has proved effective in clinical practice, particularly for the treatment of B cell leukemia⁴⁸. Along the same lines, naked monoclonal antibodies have also been developed for the specific treatment of AML by targeting several antigens expressed on blasts, including, in particular, CD33 (refs. 49, 50), CD123 (refs. 12, 13) and, more anecdotally, CD135 (FLT-3) and CXCR4 (ref. 51). All these antibodies displayed some efficacy and functionality in preclinical studies and early clinical trials, but none was considered sufficiently potent in later phases of testing to become the standard of care for AML. In this study, we found that the expression of high-affinity FcγR CD64 on AML blasts interfered with the ADCC mediated by anti-CD123 antibodies. This observation was confirmed by results for other antigens (Extended Data Fig. 4a,b). Based on 3D-structure data for IgG1-Fc complexed with CD16a (ref. 52) and CD64 (ref. 53), showing that both molecules interact

with overlapping binding sites on the Fc and given the three orders of magnitude higher affinity of binding to human IgG1 for CD64 than for CD16a (Extended Data Table 1), we hypothesized that the *cis* capture of antibody Fc at the blast cell surface by CD64 might prevent the binding of antibody Fc in *trans* to CD16a on NK cells, leading to the abolition of ADCC. The 3D-structures of IgG1-Fc complexed with CD32 (ref. 54) and the complement factor C1q (ref. 55) also revealed a highly probable competitive mode of binding to CD64, suggesting that CD64 expression may also protect cancer cells from antibody-dependent cell phagocytosis and complement-dependent cytotoxicity. A substantial proportion of patients with AML (about 30%) express CD64 on their blasts^{38,39}. CD64 expression probably therefore protects cancer cells from ADCC, and potentially complement-dependent cytotoxicity and antibody-dependent cell phagocytosis *in vivo*, explaining the disappointingly low efficacy of antibodies acting via these modes of action in the treatment of patients with AML.

We report here the preclinical development of a new antibody-based NK cell engager technology, CD123-NKCE, targeting CD123 on malignant cells and coengaging CD16a and NKp46 on NK cells. We show that redirecting NK cells against cancer targets through binding to NKp46 circumvents the CD64-mediated inhibition of ADCC, with CD123-NKCE active and superior to Fc-engineered ADCC-enhancing IgG1 antibody targeting the same antigen, *in vitro*, *ex vivo* and *in vivo*, whatever the CD64 status of the target cells. Moreover, through their binding to NKp46, CD123-NKCE specifically target NK cells, a population of effector cells with promising perspectives for use in the treatment of cancer^{15–18}, in terms of both efficacy and safety. The efficacy of CD123-NKCE to deplete CD123-positive cells *ex vivo* from human PBMCs and *in vivo* in NHP was not associated with the induction of strong cytokine release or clinical signs of toxicity. The activity, safety, pharmacokinetic and pharmacodynamics data provided here thus demonstrate the superiority of CD123-NKCEs over comparator cytotoxic antibodies in terms of antitumor activity, and their favorable safety profiles relative to T cell therapies for the treatment of AML.

Online content

Any methods, additional references, Nature Portfolio reporting summaries, source data, extended data, supplementary information, acknowledgements, peer review information; details of author contributions and competing interests; and statements of data and code availability are available at <https://doi.org/10.1038/s41587-022-01626-2>.

References

- Dohner, H., Weisdorf, D. J. & Bloomfield, C. D. Acute myeloid leukemia. *New Engl. J. Med.* **373**, 1136–1152 (2015).
- De Kouchkovsky, I. & Abdul-Hay, M. Acute myeloid leukemia: a comprehensive review and 2016 update. *Blood Cancer J.* **6**, e441 (2016).
- Tamamy, G. et al. Frontline treatment of acute myeloid leukemia in adults. *Critical Rev. Oncol. Hematol.* **110**, 20–34 (2017).
- Mahalleh, M., Shabani, M., Rayzan, E. & Rezaei, N. Reinforcing the primary immunotherapy modulators against acute leukemia; monoclonal antibodies in AML. *Immunotherapy* **11**, 1583–1600 (2019).
- Uy, G. L. et al. Flotetuzumab as salvage immunotherapy for refractory acute myeloid leukemia. *Blood* **137**, 751–762 (2021).
- Subklewe, M. et al. Preliminary results from a phase 1 first-in-human study of AMG 673, a novel half-life extended (HLE) anti-CD33/CD3 BiTE[®] (Bispecific T-Cell Engager) in patients with relapsed/refractory (R/R) acute myeloid leukemia (AML). *Blood* **134**, 833–833 (2019).
- Liu, F. et al. First-in-human CLL1-CD33 compound CAR T cell therapy induces complete remission in patients with refractory acute myeloid leukemia: update on Phase 1 clinical trial. *Blood* **132**, 901–901 (2018).

8. Epperly, R., Gottschalk, S. & Velasquez, M. P. Harnessing T cells to target pediatric acute myeloid leukemia: CARs, BiTEs, and beyond. *Children* **7**, 14 (2020).
9. Testa, U. et al. Elevated expression of IL-3Ralpha in acute myelogenous leukemia is associated with enhanced blast proliferation, increased cellularity, and poor prognosis. *Blood* **100**, 2980–2988 (2002).
10. Testa, U., Pelosi, E. & Frankel, A. CD 123 is a membrane biomarker and a therapeutic target in hematologic malignancies. *Biomark. Res.* **2**, 4 (2014).
11. Jordan, C. T. et al. The interleukin-3 receptor alpha chain is a unique marker for human acute myelogenous leukemia stem cells. *Leukemia* **14**, 1777–1784 (2000).
12. He, S. Z. et al. A phase 1 study of the safety, pharmacokinetics and anti-leukemic activity of the anti-CD123 monoclonal antibody CSL360 in relapsed, refractory or high-risk acute myeloid leukemia. *Leuk. Lymphoma* **56**, 1406–1415 (2015).
13. Montesinos, P. et al. Safety and efficacy of talacotuzumab plus decitabine or decitabine alone in patients with acute myeloid leukemia not eligible for chemotherapy: results from a multicenter, randomized, phase 2/3 study. *Leukemia* **35**, 62–74 (2021).
14. Sun, Y., Wang, S., Zhao, L., Zhang, B. & Chen, H. IFN-gamma and TNF-alpha aggravate endothelial damage caused by CD123-targeted CAR T cell. *OncoTargets Ther.* **12**, 4907–4925 (2019).
15. Berrien-Elliott, M. M., Wagner, J. A. & Fehniger, T. A. Human cytokine-induced memory-like natural killer cells. *J. Innate Immun.* **7**, 563–571 (2015).
16. Chiossone, L. & Vivier, E. in *Oncoimmunology: A Practical Guide for Cancer Immunotherapy* (eds. Zitvogel, L. & Kroemer, G.) 275–288 (Springer, 2018).
17. Cozar, B. et al. Tumor-infiltrating natural killer cells. *Cancer Discov.* **11**, 34–44 (2021).
18. Daher, M. & Rezvani, K. Outlook for new CAR-based therapies with a focus on CAR NK cells: what lies beyond CAR-engineered T cells in the race against cancer. *Cancer Discov.* **11**, 45–58 (2021).
19. Hirayama, A. V. & Turtle, C. J. Toxicities of CD19 CAR-T cell immunotherapy. *Am. J. Hematol.* **94**, S42–S49 (2019).
20. Cerwenka, A. & Lanier, L. L. Natural killers join the fight against cancer. *Science* **359**, 1460–1461 (2018).
21. Chiossone, L., Dumas, P. Y., Vienne, M. & Vivier, E. Natural killer cells and other innate lymphoid cells in cancer. *Nat. Rev. Immunol.* **18**, 671–688 (2018).
22. Mittal, D., Vijayan, D. & Smyth, M. J. Overcoming acquired PD-1/PD-L1 resistance with CD38 blockade. *Cancer Discov.* **8**, 1066–1068 (2018).
23. Demaria, O., Gauthier, L., Debroas, G. & Vivier, E. Natural killer cell engagers in cancer immunotherapy: next generation of immuno-oncology treatments. *Eur. J. Immunol.* **51**, 1934–1942 (2021).
24. Moretta, A. et al. Receptors for HLA class-I molecules in human natural killer cells. *Ann. Rev. Immunol.* **14**, 619–648 (1996).
25. Moretta, L. et al. Surface NK receptors and their ligands on tumor cells. *Semin. Immunol.* **18**, 151–158 (2006).
26. Wu, N. & Veillette, A. SLAM family receptors in normal immunity and immune pathologies. *Curr. Opin. Immunol.* **38**, 45–51 (2016).
27. Bryceson, Y. T., Ljunggren, H. G. & Long, E. O. Minimal requirement for induction of natural cytotoxicity and intersection of activation signals by inhibitory receptors. *Blood* **114**, 2657–2666 (2009).
28. Bryceson, Y. T., March, M. E., Ljunggren, H. G. & Long, E. O. Activation, coactivation, and costimulation of resting human natural killer cells. *Immunol. Rev.* **214**, 73–91 (2006).
29. Gauthier, L. et al. Multifunctional natural killer cell engagers targeting NKp46 trigger protective tumor immunity. *Cell* **177**, 1701–1713 (2019).
30. Demaria, O., Gauthier, L., Debroas, G. & Vivier, E. Natural killer cell engagers in cancer immunotherapy: next generation of immuno-oncology treatments. *Eur. J. Immunol.* **51**, 1934–1942 (2021).
31. Sivori, S. et al. p46, a novel natural killer cell-specific surface molecule that mediates cell activation. *J. Exper. Med.* **186**, 1129–1136 (1997).
32. Vivier, E. et al. Innate lymphoid cells: 10 years on. *Cell* **174**, 1054–1066 (2018).
33. Sivori, S. et al. NKp46 is the major triggering receptor involved in the natural cytotoxicity of fresh or cultured human NK cells. Correlation between surface density of NKp46 and natural cytotoxicity against autologous, allogeneic or xenogeneic target cells. *Euro. J. Immunol.* **29**, 1656–1666 (1999).
34. Crinier, A., Escalière, B., Narni-Mancinelli, E. & Vivier, E. Reply to ‘Comment to: single-cell profiling reveals the trajectories of natural killer cell differentiation in bone marrow and a stress signature induced by acute myeloid leukemia’. *Cell. Mol. Immunol.* **18**, 1350–1352 (2021).
35. Fauriat, C. et al. Deficient expression of NCR in NK cells from acute myeloid leukemia: evolution during leukemia treatment and impact of leukemia cells in NCRdull phenotype induction. *Blood* **109**, 323–330 (2007).
36. Rey, J. et al. Kinetics of cytotoxic lymphocytes reconstitution after induction chemotherapy in elderly AML patients reveals progressive recovery of normal phenotypic and functional features in NK cells. *Front. Immunol.* **8**, 64 (2017).
37. Chretien, A. S. et al. NKp46 expression on NK cells as a prognostic and predictive biomarker for response to allo-SCT in patients with AML. *Oncoimmunology* **6**, e1307491 (2017).
38. Gupta, N. et al. Spectrum and immunophenotypic profile of acute leukemia: a tertiary center flow cytometry experience. *Med. J. Hematol. Infect. Dis.* **11**, e2019017 (2019).
39. Heitmann, J. S. et al. Fc gamma receptor expression serves as prognostic and diagnostic factor in AML. *Leuk. Lymphoma* **61**, 2466–2474 (2020).
40. Bournazos, S., Wang, T. T. & Ravetch, J. V. in *Myeloid Cells in Health and Disease* (ed. Gordon, S.) 405–427 (Wiley, 2017).
41. Jin, L. et al. Monoclonal antibody-mediated targeting of CD123, IL-3 receptor alpha chain, eliminates human acute myeloid leukemic stem cells. *Cell Stem Cell* **5**, 31–42 (2009).
42. Xie, L. H. et al. CD123 target validation and preclinical evaluation of ADCC activity of anti-CD123 antibody CSL362 in combination with NKs from AML patients in remission. *Blood Cancer J.* **7**, e567–e567 (2017).
43. Walzer, T. et al. Identification, activation, and selective in vivo ablation of mouse NK cells via NKp46. *Proc. Natl Acad. Sci. USA* **104**, 3384–3389 (2007).
44. Chichili, G. R. et al. A CD3xCD123 bispecific DART for redirecting host T cells to myelogenous leukemia: preclinical activity and safety in nonhuman primates. *Sci. Transl. Med.* **7**, 289ra282 (2015).
45. US FDA. Points to consider in the manufacture and testing of monoclonal antibody products for human use (1997). US Food and Drug Administration center for biologics evaluation and research. *J. Immunother.* **20**, 214–243 (1997).
46. Busfield, S. J. et al. Targeting of acute myeloid leukemia in vitro and in vivo with an anti-CD123 mAb engineered for optimal ADCC. *Leukemia* **28**, 2213–2221 (2014).
47. Barrett, A. J. Antibody darts on target for acute myelogenous leukemia. *Ann. Transl. Med.* **5**, 80 (2017).
48. Freeman, C. L. & Sehn, L. H. A tale of two antibodies: obinutuzumab versus rituximab. *Br. J. Haematol.* **182**, 29–45 (2018).

49. Walter, R. B. Investigational CD33-targeted therapeutics for acute myeloid leukemia. *Expert Opin. Investig. Drugs* **27**, 339–348 (2018).
50. Feldman, E. J. et al. Phase III randomized multicenter study of a humanized anti-CD33 monoclonal antibody, lintuzumab, in combination with chemotherapy, versus chemotherapy alone in patients with refractory or first-relapsed acute myeloid leukemia. *J. Clin. Oncol.* **23**, 4110–4116 (2005).
51. Becker, P. S. et al. Targeting the CXCR4 pathway: safety, tolerability and clinical activity of ulocuplumab (BMS-936564), an anti-CXCR4 antibody, in relapsed/refractory acute myeloid leukemia. *Blood* **124**, 386–386 (2014).
52. Sondermann, P., Huber, R., Oosthuizen, V. & Jacob, U. The 3.2-A crystal structure of the human IgG1 Fc fragment-Fc gammaRIII complex. *Nature* **406**, 267–273 (2000).
53. Lu, J. et al. Structure of FcγRI in complex with Fc reveals the importance of glycan recognition for high-affinity IgG binding. *Proc. Natl Acad. Sci. USA* **112**, 833–838 (2015).
54. Ramsland, P. A. et al. Structural basis for Fc gammaRIIIa recognition of human IgG and formation of inflammatory signaling complexes. *J. Immunol.* **187**, 3208–3217 (2011).
55. Ugurlar, D. et al. Structures of C1-IgG1 provide insights into how dangerpattern recognition activates complement. *Science* **359**, 794–797 (2018).

Publisher's note Springer Nature remains neutral with regard to jurisdictional claims in published maps and institutional affiliations.

Open Access This article is licensed under a Creative Commons Attribution 4.0 International License, which permits use, sharing, adaptation, distribution and reproduction in any medium or format, as long as you give appropriate credit to the original author(s) and the source, provide a link to the Creative Commons license, and indicate if changes were made. The images or other third party material in this article are included in the article's Creative Commons license, unless indicated otherwise in a credit line to the material. If material is not included in the article's Creative Commons license and your intended use is not permitted by statutory regulation or exceeds the permitted use, you will need to obtain permission directly from the copyright holder. To view a copy of this license, visit <http://creativecommons.org/licenses/by/4.0/>.

© The Author(s) 2023

Methods

NKCE expression and purification

The sequences encoding each polypeptide chain of the NKCE molecules were inserted into the pTT-5 vector between the *HindIII* and *BamHI* restriction sites, as described previously²⁹. The three vectors were used to cotransfect EXPI-293F cells (ThermoFisher Scientific, 100044202) in the presence of PEI (37 °C, 5% CO₂, shaking at 150 rpm). Cells were seeded at a density of 10⁶ cells per ml in EXPI293 medium (Gibco, A1435101) supplemented with valproic acid (0.5 mM), glucose (4 g l⁻¹) and tryptone NI (0.5%), and cultured for 6 days. NKCE molecules were purified with rProtein A Sepharose Fast Flow resin (GE Healthcare, 17-1279-03), followed by cation ion exchange chromatography onto two HiTrap SP-HP 1 ml columns (GE Healthcare, 17-1151-01) in series and finally dialyzed overnight against 1× PBS. The CD123-NKCE batch used for the NHP study was produced at Sanofi in a 200 l bioreactor with a CHO stable-producer clone, and purified according to the Sanofi process development platform procedure.

Recombinant protein cloning, production and purification

The human and cynomolgus recombinant proteins listed below were produced and purified at Innate Pharma as described previously²⁹: human NKp46 (Gln22-Asn255, National Center for Biotechnology Information (NCBI) [NM_004829.5](#)), human neonatal Fc receptor (FcRn, NCBI [P55899](#)), human CD16a (human FcγRIIIA V and F isoforms, NCBI [AAH36723](#)), human CD32a (human FcγRIIA, NCBI [AAH20823](#)), human CD32b (human FcγRIIB, NCBI [NP_003992](#)), human CD16b (human FcγRIIIB, NCBI [AAI28563](#)), human CD64 (human FcγRI, NCBI [P12314](#)), cynomolgus NKp46 (Gln17-Asn254, NCBI [NP_001271509.1](#)), cynomolgus FcRn (NCBI [Q8SPV9](#)), cynomolgus CD16 (NCBI [NP_001270121.1](#)), cynomolgus CD32a (NCBI [NP_001270598.1](#)), cynomolgus CD32b (NCBI reference [NP_001271060.1](#)) and cynomolgus CD64 (NCBI [AAL92095.1](#)). The recombinant human CD123 was purchased from ACRO Biosystems (ILA-H52H6).

Surface plasmon resonance study of binding

A Biacore T200 instrument (Cytiva, 28975001) was used with Series S CM5 sensor chips (Cytiva, 29149603) and experiments were performed at 25 °C.

Affinity capture of the NKCE sample was achieved with the human antibody capture kit (Cytiva, BR1008-39). Seven serial 1:1 dilutions of either human and cynomolgus NKp46 or human CD123 in HBS-EP + buffer (Cytiva, BR1006-69) were prepared at concentrations of ranging from 1.56 to 100 nM. The CD123-NKCE (0.06 μg ml⁻¹) was captured on the anti-Fc chip at a flow rate of 10 μl min⁻¹ for 90 s to yield maximal response (R_{max}) values of approximately 30 RU. Proteins were injected for 240 s at a flow rate of 30 μl min⁻¹ onto captured NKCE, followed by a dissociation phase of 1,200 s. All analyte concentrations were run in duplicate, together with multiple buffer blanks for double referencing. The capture surface was regenerated with regeneration solution (3 mol l⁻¹ MgCl₂) at a flow rate of 30 μl min⁻¹ for 60 s. The data were evaluated with Biacore T200 Evaluation Software v.3.0 (Cytiva) using a 1:1 binding model with a mass transport limitation.

For FcR binding studies, CD123-NKCE molecules and control human IgG1 antibodies were immobilized (at about 700 RU) onto the dextran layer of a CM5 Series S sensor chip on flow cells 2 and 3 by amine coupling chemistry. Flow cell 1 activated with NHS/EDC alone and deactivated with ethanolamine served as a reference flow cell for online blank subtraction.

For all experiments other than the FcRn binding study, HBS-EP⁺ 1× was used as the running buffer. For the FcRn binding study, acetate buffer pH 5.6 replaced HBS-EP⁺. Serial dilutions of FcRn and FcγRs were sequentially injected over a period of 2 min, at a constant flow rate of 40 μl min⁻¹ over the CM5 chip and allowed to dissociate for 10 min before regeneration (10 s of 10 mM NaOH 500 mM NaCl and 10 s of HBS-EP⁺ at a constant flow rate of 40 μl min⁻¹ for FcγRs and FcRn, respectively).

The sensorgram sets of human and cynomolgus FcγRI were fitted with the 1:1 binding model. The sensorgram sets of human FcγRIIA, FcγRIIB, FcγRIIIaF, FcγRIIIaV and FcγRIIIB, and cynomolgus FcγRIIA, FcγRIIB and FcγRIII were fitted with a steady-state affinity model.

The sensorgram sets of human and cynomolgus FcRn were fitted with a two-state reaction model. The experiment was performed three times, on three different days, with the same Biacore CM5 chip. The affinities for human and cyno FcRn and FcγRI were calculated from the kinetic association (k_a) and dissociation (k_d) rate constants: dissociation constant (K_D) = k_d/k_a .

Affinities for human and cynomolgus FcγRII and FcγRIII receptors were calculated from Scatchard plot fits.

Biological samples

Healthy human buffy coats were provided by the Etablissement Français du Sang (EFS, the French blood service, Marseille; AC-2019-3428). Peripheral mononuclear cells (PBMC) were isolated from buffy coats by Ficoll density gradient centrifugation. Human NK cells were purified from PBMCs with a bead-based negative selection kit (Miltenyi, 130-092-657). Samples from patients with AML were provided by Institut Paoli-Calmettes (Marseille, SA-IPH-IMAbs Contract).

Cell lines

KG-1a, Kasumi-6, GDM-1, MOLM-13 and THP-1 AML cell lines were purchased at ATCC. M-07e, EOL-1, Kasumi-1, F36-P, NB-4, OCI-AML2, MV4-11, OCI-AML3 and SKM-1 AML cell lines were purchased at DSMZ. Cells were cultured in Roswell Park Memorial Institute (RPMI)-1640 medium supplemented with 10% FBS, 2 mM L-glutamine, 1 mM sodium pyruvate and 1× nonessential amino acids (complete RPMI). Culture medium was supplemented with 25 mM HEPES for THP-1 cells. Quantification of CD123 expression on AML cell lines (antibody binding capacity) was performed by flow cytometry using mouse IgG calibrator kit (BioCytex, CP051). Anti-CD123 antibody 9F5 and isotype control (BD Biosciences, 555642 and 553447) were used at saturating concentration (10 μg ml⁻¹) for the quantification. CD64 and CD32a/b expression in THP-1 cells was silenced with CRISPR-Cas9 endonucleases. For the generation of CD64-deficient THP-1 cells (THP-1 CD64-KO), 2.5 × 10⁶ cells were nucleofected (Neon Transfection System, 100 μl tip, 1,700 V, 20 ms, one pulse) with two sgRNAs (CD64.1: CUUGAGGUGUCAUGCGUGGA; CD64.2: AAGCAUCGCUACAUCAGC; Synthego) at a Cas9:sgRNA ratio of 1:9 (Alt-R-S.p. Cas9 Nuclease 3NLS, Integrated DNA Technology). For the generation of CD32-deficient THP-1 cells (THP-1 CD32-KO), 2.5 × 10⁶ cells were nucleofected with two sgRNAs (CD32A, AUGUAUGUCCCA-GAAACCUG; CD32B, AAGCAUAUGACCCCAAGGCU; Integrated DNA Technologies) at a Cas9:sgRNA ratio of 1:9. Absence of CD64 and CD32 expression was confirmed by flow cytometry and cells were either sorted or subcloned.

NK cell-based cytotoxic assay

For cytotoxic assays performed on AML cell lines (that is, KG-1a, M-07e, EOL-1, Kasumi-1, F36-P, Kasumi-6, GDM-1, NB-4, OCI-AML2, MV4-11, OCI-AML3, SKM-1, MOLM-13, THP-1 or THP-1 CD64-KO, THP-1 CD32-KO), target cells were loaded with Cr-51.

Seven primary samples from patients with AML collected at diagnosis were used for the study. They were composed by PBMC and AML blasts. The day before the cytotoxic assay, primary samples were thawed, cells were counted with a trypan blue exclusion test and cultured in complete RPMI at 2 × 10⁶ cells per ml. The viability of primary AML cells was monitored at each step of the experimental process. Primary cells AML samples were loaded with CalceinAM (8 μg ml⁻¹; Life Technologies, C3100MP) for 30 min in the presence of 2.5 mM probenecid (ThermoFisher, P36400). Dilution ranges of both test and control items from 5 to 2.10⁻⁵ μg ml⁻¹ (1/12 serial dilution) and 5 to 5.10⁻⁷ μg ml⁻¹ (1/10 serial dilution) were performed for experiments with primary AML cells or AML cell lines, respectively.

Antibodies, target cells (roughly 3,000 cells) and human NK cells (roughly 30,000 cells) were successively added to each well of round-bottomed 96-well plates. After 4 h of coincubation, the supernatant was transferred to a Lumaplate (for Cr-51) or a flat-bottomed culture plate (for CalceinAM).

Cr-51 released from dead target cells was determined with a Top-Count NXT (Microplate Scintillation and Luminescence Counter; Perkin Elmer). Radioactivity was measured by counting γ -emission for 60 s for each well. The results are expressed in cpm (counts per minute). CalceinAM released by dead target cells was determined by measuring the number of relative fluorescence units (RFU) with a luminometer (EnSpire Multimode Plate Reader, Perkin Elmer; excitation at $\lambda = 495$ nm and emission at $\lambda = 516$ nm). The percentage specific lysis was calculated with the following formula:

Specific lysis (%) = $(ER \text{ (cpm or RFU)} - SR \text{ (cpm or RFU)}) / (MR \text{ (cpm or RFU)} - SR \text{ (cpm or RFU)}) \times 100$ where ER = experimental release, SR = spontaneous release and MR = maximal release.

EC₅₀ were determined by fitting the data with nonlinear regression curve model (log(agonist) versus response-variable slope (four parameters)) with GraphPad Prism Software v.8.0.2.

NK cell degranulation assay with AML samples

Tested items and PBMCs from patients with AML were added to each well of round-bottomed 96-well plates. After overnight coincubation with the NKCE molecules or antibodies, antihuman CD107a and CD107b antibodies (Miltenyi, 130-111-621 and 130-118-818) were added for 4 h. Cells were then washed and stained with the following mixture: viability markers, anti-CD45 (Miltenyi, 130-110-771), anti-CD33 (BD Biosciences, 564588), anti-CD56 (BD Biosciences, 557747) and anti-CD3 (BD Biosciences, 740187) antibodies. Cells were then washed, fixed and analyzed by flow cytometry. The data obtained were analyzed with FlowJo Software to assess NK cell degranulation by monitoring the expression of CD107a/b on NK cells identified as living CD45⁺CD33⁺CD56⁺CD3⁻ cells.

NK cell activation assay with AML cell lines

A dilution range from 15 to 15.10⁻⁷ $\mu\text{g ml}^{-1}$ (1/10e serial dilution) was performed for both test and control items. The tested items, MOLM-13 cells (roughly 50,000 cells) and human NK cells (roughly 50,000 cells) from healthy donors were successively added to each well of round-bottomed 96-well plates. Control conditions were performed by adding only 50,000 resting NK cells by well. BD GolgiSTOP solution (BD Biosciences, 554724) was added at a final dilution of 1/6,000 in each well. A positive control of NK cell activation was performed by using Phorbol 12-myristate 13-acetate (PMA, 125 ng ml⁻¹ final; SIGMA, P8139) and of Ionomycin (IONO, 1 $\mu\text{g ml}^{-1}$ final; SIGMA, I0634) added on 50,000 NK cells. Each condition was performed in triplicate. After 4 h of coincubation at 37 \pm 1 °C and 5 \pm 1% CO₂, an extracellular staining was performed for CD3, CD56, CD107a and CD107b (Human NK cell activation panel cocktail; Miltenyi, 130-095-212) and CD69 (Miltenyi, 130-113-523). An intracellular staining was performed for IFN- γ (Biolegend, 502536), TNF- α (BD Biosciences, 563996) and MIP-1 β (BD Biosciences, 550078). Cells were analyzed by flow cytometry (Supplementary Fig. 3). Parameters were recorded with BD FACSDiva v.8.0 software and the analyses were done with FlowJo v10.5.2 software. Analysis of the percentage of NK cell activation was done with GraphPad prism v.8.0.2.

In vitro pharmacodynamic assessment and cytokine release in human PBMC

PBMCs from human healthy donors ($n = 10$) were seeded in 190 μl complete culture medium (500,000 cells per well) in 96-well U-bottomed plates (Costar, Ultra low binding CLS7007), and incubated at 37 °C and 5% CO₂ for 20 h in presence of serial dilutions of CD123-NKCE, IC-NKCE control or CD123-TCE molecules. The basophil population, defined as

TCR $\alpha\beta$ CD14⁺IgE⁺ viable cells, was analyzed by flow cytometry and the absolute concentrations of cytokines released into the supernatant were analyzed by mesoscale discovery (MSD) assay.

For flow cytometry analysis, cell pellets were suspended in cold 50 μl staining buffer (Miltenyi, AutoMACS Running Buffer 130-091-221) supplemented with 1 μl of human FcR blocking reagent (Miltenyi, 130-059-901). A mixture of PBMC subset-specific antibodies and the viability reagent were added to the PBMC suspension according to the supplier's instructions. As a fluorescence minus one control, additional points were obtained by labeling PBMC with the same mixture, but with each labeling antibody replaced in turn by its corresponding isotype control. Cells and antibody mixtures were incubated for 1 h at 4 °C in the dark, and then washed twice with 200 μl of staining buffer by centrifugation at 300g for 5 min at 4 °C. Cells were analyzed with a MACSQuant Analyzer from Miltenyi Biotec. Raw data were analyzed with VenturiOne v.6.1 software (Applied Cytometry Inc.). The gating strategy can be found in Supplementary Fig. 4.

For MSD assay, cell supernatant was diluted in MSD buffer following the manufacturer's instructions. Diluted samples or prediluted multi-analyte calibrator samples were added to the precoated plate supplied in the kit. A solution of detection antibodies conjugated to electrochemiluminescent labels (MSD SULFO-TAG) was added and the plates were incubated at room temperature for 2 h before measurements. Data were analyzed with Excel 2019 software. The concentrations of IL-6, IL-1 β , IFN- γ and TNF- α were determined from electrochemiluminescent signals by back-fitting to a calibration curve established with a four-parameter logistic model with 1/Y₂ weighting.

Animal care

All animal procedures were approved by the Sanofi Animal Care and Use Committee, followed the French and European regulations on care and protection of the Laboratory Animals, and in accordance with the standards of the Association for Assessment and Accreditation of Laboratory Animal Care (AAALAC).

Antitumor activity against human MOLM-13 AML cells injected into severe combined immunodeficiency mice

The activity of the surrogate CD123-NKCE was evaluated in a disseminated human AML model consisting in MOLM-13 cells implanted in the tail vein of female severe combined immunodeficiency mice on day 0. Control groups were left untreated. Graph presented are the pooled results of four independent experiments ($n = 20$ mice per treatment group and 40 mice in the control group). Surrogate CD123-NKCE and anti-CD123 antibody were administered at doses of 5, 0.5 and 0.25 mg kg⁻¹ by intraperitoneal injections on day 1.

Mice were checked and adverse clinical reactions noted. Individual mice were weighed daily until the end of the experiment (day 70). Mice were euthanized when they were considered moribund according to pre-defined criteria, to prevent animal suffering. The disease-related clinical signs considered critical were limb paralysis, ascites, palpable internal tumor masses, morbidity or a loss of at least 20% of total body weight loss.

For NK cell depletion, 100 μl of polyclonal anti-asialo-GM1 (Poly21460, Biolegend) antibody was injected intraperitoneally into recipient mice at the indicated time points.

Pharmacodynamic activity in NHPs

A qualified flow cytometry panel composed of antibodies against the antigens CD45 (BD Biosciences ref. no. 563530, Clone D058-1283), CD14 (Miltenyi Biotec ref. no. 130-110-518, clone REA599), CD203c (Invitrogen ref. no. 17-2039, clone NP4D6), CD193 (Biolegend ref. no. 310708, clone 5E8), IgE (Miltenyi Biotec ref. no. 130-117-931, clone REA1049), CD123 (BD Biosciences ref. no. 554529, clone 7G3), CD33 (Miltenyi Biotec ref. no. 130-113-350, clone AC104.3E3) and the viability marker Zombie Nir (Biolegend ref. no. 423106) was used to evaluate the phenotype and

counts of basophils and total CD123-positive immune cells in cynomolgus monkey blood and bone marrow samples. Blood (100 μ l) and bone marrow samples (50 μ l) were collected into a K3-EDTA anticoagulation air-vacuum tubes, incubated with a lysis solution (Biocytex CP025) for 10 min and centrifuged at 300g at room temperature for 5 min with Dulbecco's PBS (Sigma D8537) before staining for 10 min, washing and fixation. We added 100 μ l of flow count beads (Beckman ref. no. A91346) to the sample before acquisition on a Beckman Coulter Gallios (single dose pharmacokinetic/pharmacodynamics study) and BD FACS Verse (repeated dose toxicity study) instruments. The gating strategy for CD123-positive immune cells can be found in Supplementary Fig. 5.

Cytokine determinations on NHP plasma

In the single dose NHP pharmacokinetic/pharmacodynamics study, a qualified electrochemiluminescence assay method was developed using the MSD V-PLEX Proinflammatory Panel NHP kit (K15056D) for the quantification of IL-2, IFN- γ , IL-6 and IL-10 in monkey K3-EDTA plasma. In the repeated dose NHP toxicity study, an exploratory electrochemiluminescence assay method was developed using the MSD U-PLEX Proinflammatory Combo1 NHP kit (K150070K-2) for the quantification of IL-6, IL-2, IL-10, TNF- α , IFN- γ , IL-1 β and IL-8 in monkey K3-EDTA plasma. Samples were analyzed according to the manufacturer's recommendations. Analyses were performed in duplicate.

Pharmacokinetic/pharmacodynamic and toxicology studies in NHPs

CD123-NKCE solutions for administration (at concentrations of 0.1, 0.6, 20 and 600 μ g ml⁻¹) were prepared extemporaneously by diluting the stock solution in vehicle. They were kept at room temperature before and during administration. We used polypropylene, polycarbonate or PETG containers for dilutions, to prevent adsorption. These containers were coated with 100 ppm PS80 in 0.9% NaCl before use. The tubing used for each i.v. administration (syringe/winged needle) was coated, by successive flushes, with a solution of 100 ppm PS80 in 0.9% NaCl. The dosing volume was 5 ml kg⁻¹ by 1 h i.v. infusion.

In the single dose pharmacokinetic/pharmacodynamics study, two males per group administered 3 or 3,000 μ g kg⁻¹ and one male administered 0.5 μ g kg⁻¹.

In the exploratory repeat-dose toxicity study, two animals per sex and per dose administered 0.1 or 3 mg kg⁻¹ per administration, once weekly, for 4 weeks (on days 1, 8, 15 and 22). One monkey per sex per dose was euthanized and necropsied 1 week after the last administration and the remaining monkeys were euthanized and necropsied at 4 weeks after the last administration. The parameters evaluated included mortality, clinical signs, body weight, injection site examination, body temperature, electrocardiography parameters, hematology, clinical chemistry, coagulation and urinalysis, macroscopic observations, organ weights and histopathologic findings.

In both studies, serial blood samples were withdrawn from the brachial or saphenous or cephalic vein into K3-EDTA polypropylene tubes for plasma CD123-NKCE concentrations, 1.5, 5, 24, 48, 72, 168, 240, 336, 504 and 672 h after the start of the infusion, for the single dose pharmacokinetic/pharmacodynamics study and predose, 1, 1.5, 5, 24, 72 and 168 h after the start of each weekly infusion for the repeated dose toxicology study. Blood samples were placed on wet ice and centrifuged. The plasma samples obtained were frozen at -80 °C until analysis.

CD123-NKCE concentrations in plasma were determined by a dedicated immunoassay method in which CD123-NKCE were captured by biotin-coupled CD123 recombinant proteins and detected with a monkey-adsorbed Alexa Fluor-conjugated-goat antihuman IgG, with a lower limit of quantification at 0.250 ng ml⁻¹.

Quantification and statistical analysis

Detailed information concerning the statistical methods used is provided in the figure legends. Statistical analyses were performed with GraphPad Prism software v.8.0.2, and v.8.3.0. Kaplan–Meier methods were used for survival analysis. When sample size was sufficiently large, the normality of populations was assessed with the d'Agostino–Pearson omnibus normality test. If the data were not normally distributed, the statistical significance of differences between paired sample populations was determined with the two-sided Wilcoxon matched-pair signed rank test. *n* is the number of samples used in the experiments. The means or medians are shown, with or without error bars indicating the s.d. Significance is indicated as follows: **P* ≤ 0.05; ***P* ≤ 0.01; ****P* ≤ 0.001, *****P* ≤ 0.0001. Four-parameter nonlinear regression analysis was used to calculate the CD123-NKCE EC₅₀.

Reporting summary

Further information on research design is available in the Nature Portfolio Reporting Summary linked to this article.

Data availability

All data supporting the results are available in the main text or the supplementary materials. The detailed molecular organization and the sequences of the NKCE used in the present study can be found in Supplementary Figs. 1 and 2, and in patents WO2016207273 and WO2022144836A1. Recombinant proteins were built from sequences found at <https://www.ncbi.nlm.nih.gov>.

Acknowledgements

We thank A. Tang, L. Bassinet and V. Boisrobert-Dheilly for performing some cellular studies, L.-M. Meyer et Ravi Rangara for animal pharmacological studies, F. Windenberger for the statistical analyses, and all members of Sanofi Immunology Research, Pharmacology, Drug Metabolism and Pharmacokinetics, Preclinical Safety, Biomarker and Clinical Bioanalysis, Large Molecule Research and Chemistry Manufacturing and Control teams who contributed to this project. We thank M. Seillier and L. Pouyet (MI-mabs, Marseille France) for performing some cellular and animal studies. We thank C. Naussac for her help in the coordination of the collaborative work. The study was performed and supported by two private companies, namely Sanofi and Innate Pharma, without the help of any funder or grant.

Author contributions

L.G., A.V.-O., M.C. and Y.M. initiated and designed the study. M.A. contributed to the initiation of the study and coordinated the collaborative work. L.G., A.V.-O., J.B. M.C., Y.M., and E.V. supervised the study, provided analysis and advices. L.G. and E.V. wrote the manuscript with the help of A.V.-O., M.C. and the other coauthors. L.G., A.V.-O., J.B., B.R., C.N., C.A., A.B.-A., N.G., J.C., A.B., F.G., G.G., H.B., A.-L.B. and A.M. performed the experiments and/or analyzed and/or interpreted results.

Competing interests

L.G., B.R., A.B.-A., N.G., F.G., G.G., A.M., Y.M. and E.V. are employees of Innate Pharma. A.V.-O., M.C., M.A., J.B., C.N., C.A., J.C., A.B., H.B. and A.-L.B. are employees of SANOFI. L.G., B.R., A.M., A.V.-O., M.C., C.N., C.A. and J.B. hold patents related to multifunctional antibodies engaging NK cells (WO2022144836A1).

Additional information

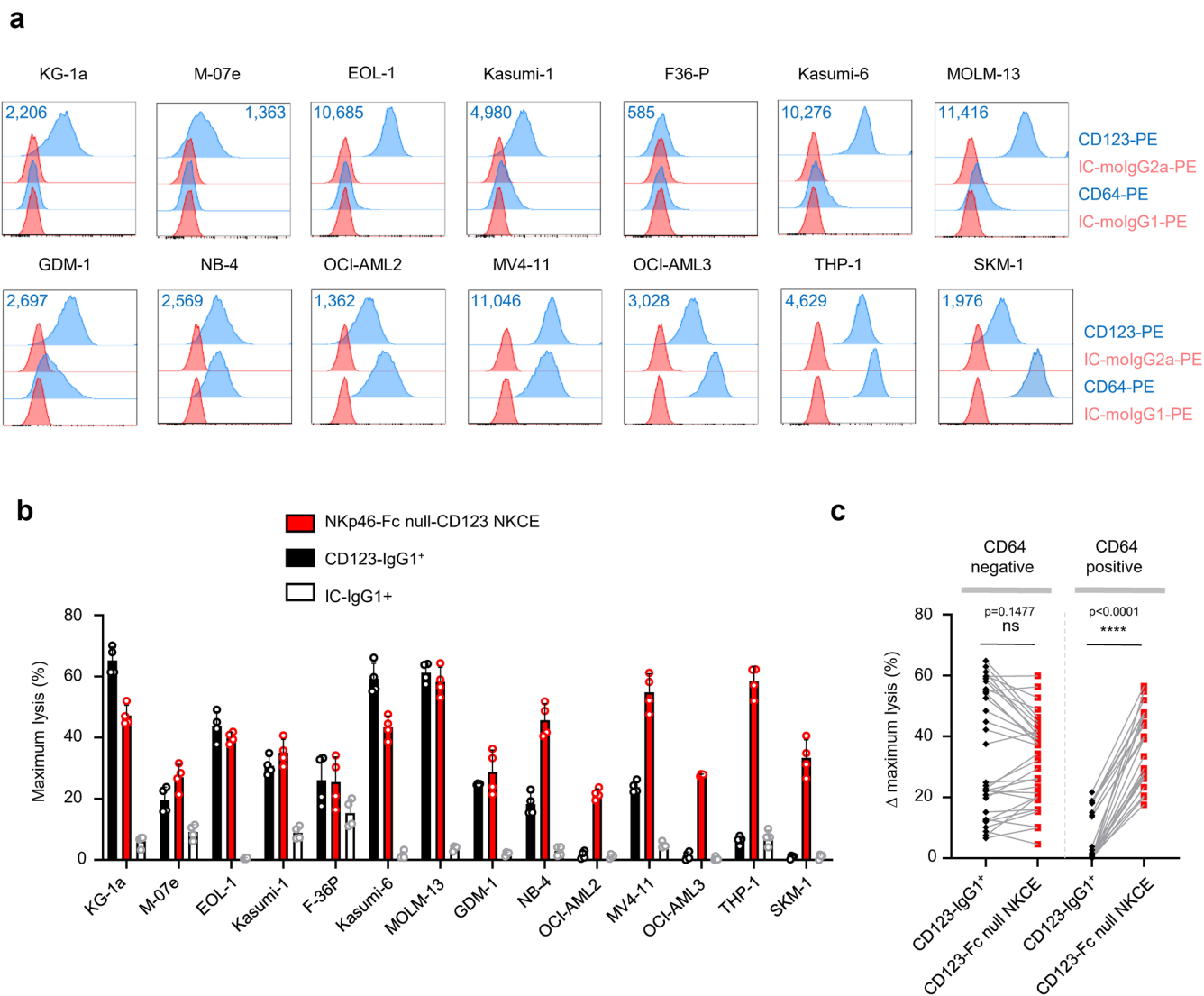
Extended data is available for this paper at <https://doi.org/10.1038/s41587-022-01626-2>.

Supplementary information The online version contains supplementary material available at <https://doi.org/10.1038/s41587-022-01626-2>.

Correspondence and requests for materials should be addressed to Laurent Gauthier, Angela Virone-Oddos or Eric Vivier.

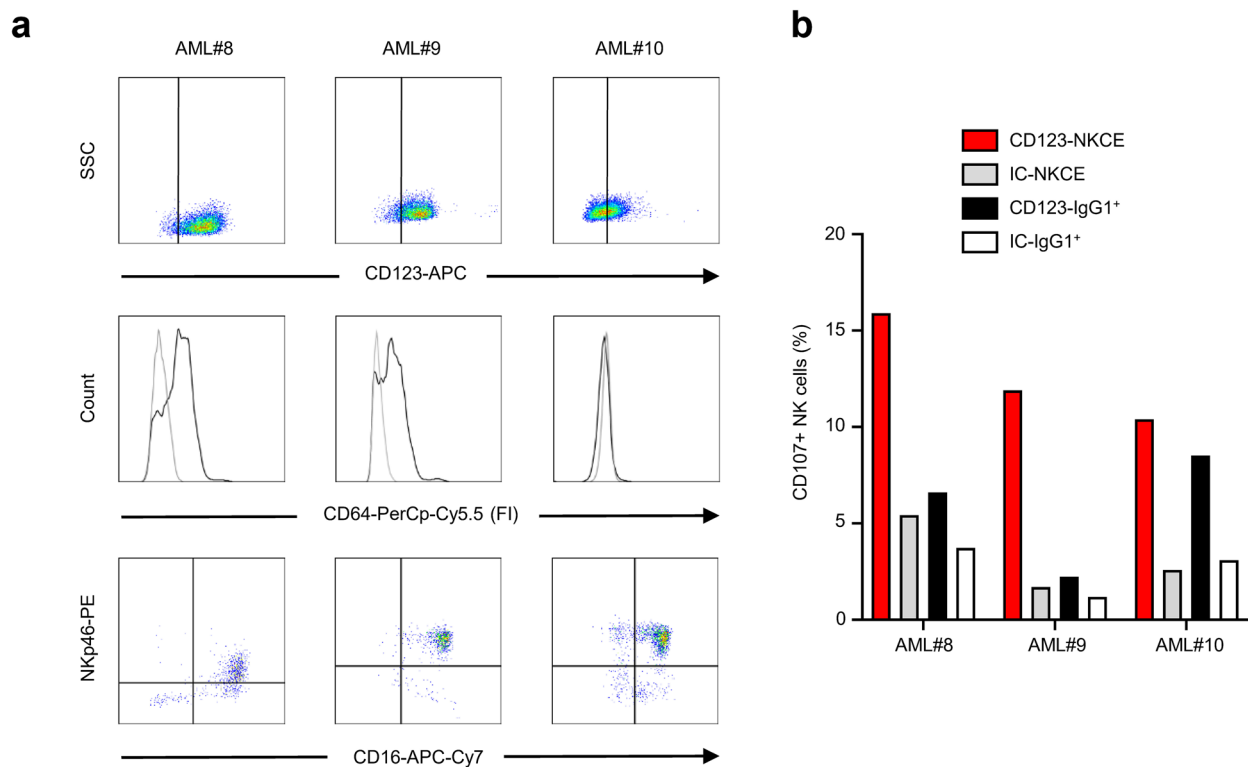
Peer review information *Nature Biotechnology* thanks the anonymous reviewers for their contribution to the peer review of this work.

Reprints and permissions information is available at www.nature.com/reprints.



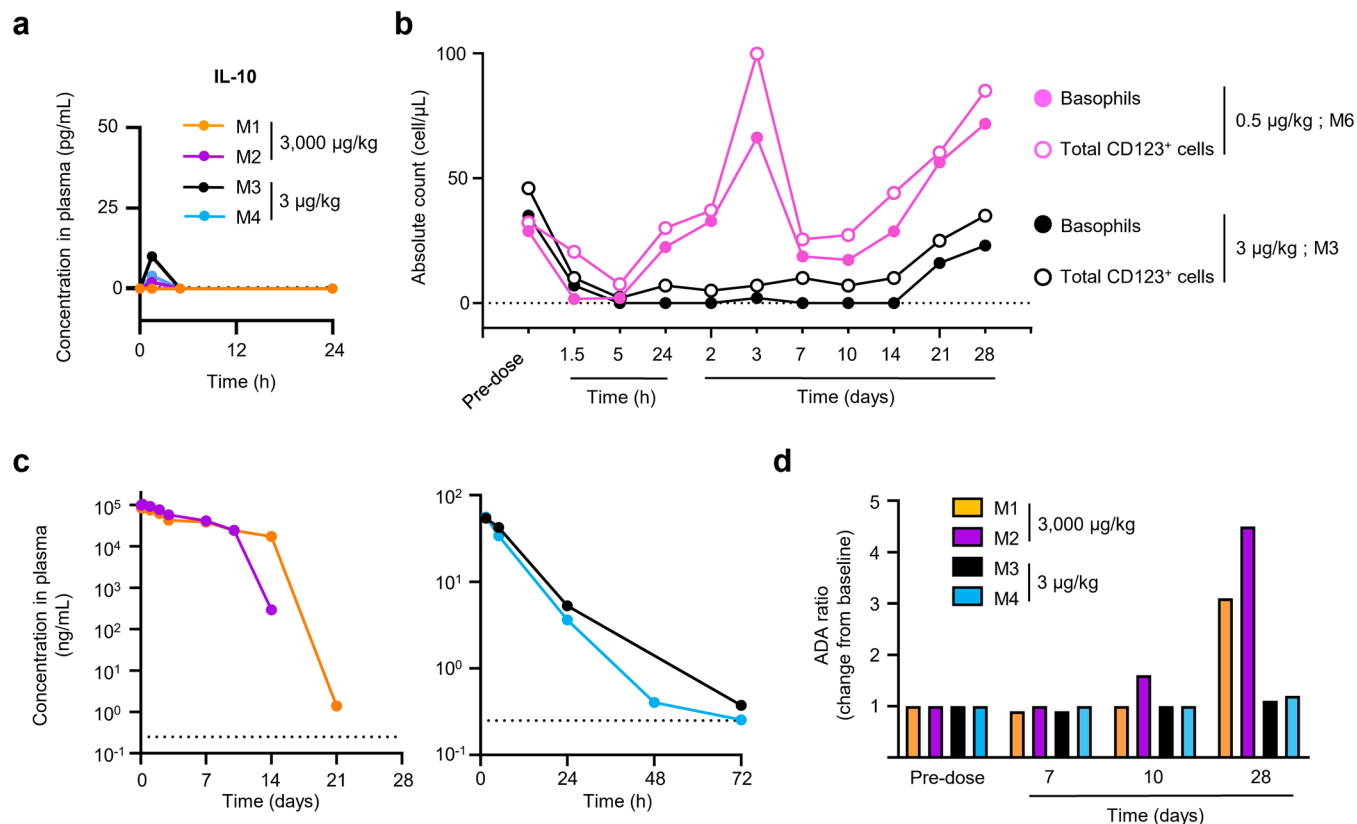
Extended Data Fig. 1 | CD123⁺ NKCE promotes strong killing activity against AML cells that is not affected by the expression of CD64. **a**, Phenotype of the 14 AML cell lines used in the study showing the expression of CD64 and CD123 at the cell surface by flow cytometry. Antibody binding capacity (ABC) values for CD123 are indicated. **b**, Maximum cytotoxic activities of the anti-CD123 antibody (CD123-IgG1⁺; black), NKp46-Fc null-CD123 NKCE (red), and IgG1 isotype control (IC-IgG1⁺; white) against AML cell lines. AML cell lines were used as targets

and purified NK cells from 4 healthy donors were used as effectors. Data are presented as mean values \pm s.d. **c**, Delta (Δ) maximum lysis, defined as percent maximum lysis of the compound minus percent background lysis of the isotype control molecule (IC-IgG1⁺) at the corresponding concentration, were monitored from the dose response of each compound, and were plotted separately for all couples of CD64⁺ positive and CD64⁻ negative AML cell lines/NK donor. (ns $P > 0.05$; **** $P \leq 0.0001$; two-sided Wilcoxon matched-pairs signed rank test).



Extended Data Fig. 2 | CD123⁺ NKCE-mediated activation of autologous NK-cells against AML blasts is not affected by the expression of CD64.
a, Phenotypes of NK and malignant cells from AML patients. *Upper panels*, Expression of CD123 on AML blasts (gated on the CD33⁺ positive population); *middle panels*, expression of CD64 (CD64 staining in black and isotype control

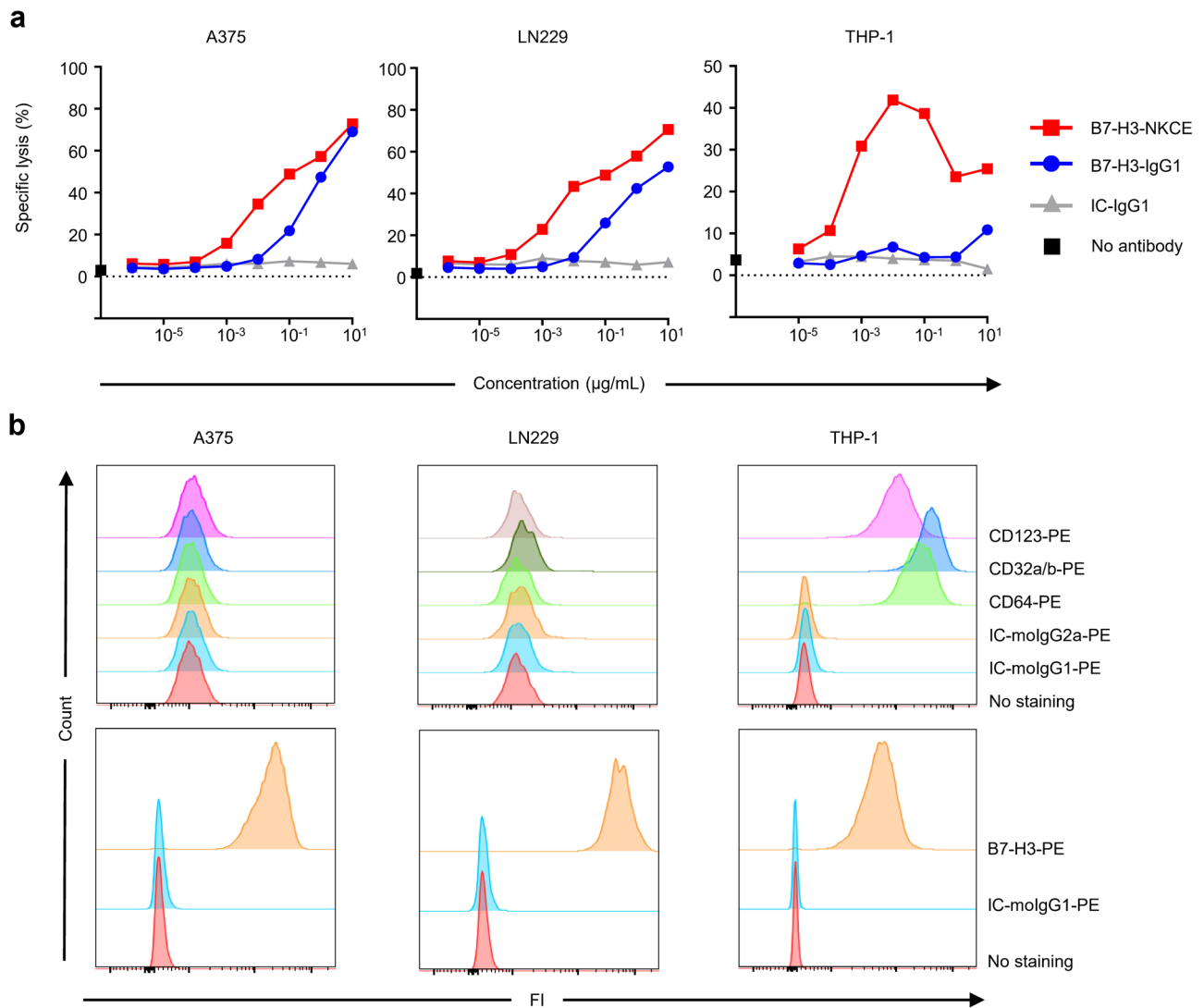
in gray) on CD123-positive AML blasts; *lower panels*, expression of NKp46 and CD16a on AML sample NK cells. **b**, Measurement, by flow cytometry, of CD107a/b expression by NK cells after the overnight treatment of PBMCs from AML patients with 120 ng/mL CD123-NKCE (red), anti-CD123 antibody (CD123-IgG1⁺; black), and IC-IgG1⁺ (white) and IC-NKCE (gray) negative control molecules.



Extended Data Fig. 3 | CD123-NKCE is safe and induces pharmacodynamic effects through the sustained depletion of CD123-positive cells in NHPs.

a, Cytokine production in cynomolgus monkeys treated with the high and low doses of 3 mg/kg and 3 μg/kg as single 1-hour intravenous infusion, respectively. Plasma IL-10 concentrations are shown before dosing (0), and 1.5, 5 and 24 hours after the start of the treatment. **b**, Numbers of circulating CD123-positive basophils (close symbols) and total CD123-positive leukocytes (open symbols) at time of study in monkeys M6 (pink) and M3 (black) treated with 0.5 and 3 μg/kg as single 1-hour intravenous infusion, respectively. **c**, Pharmacokinetics of the CD123-NKCE molecule in monkeys M1 (orange) and M2 (purple) treated with

3 mg/kg (left panel), and monkeys M3 (black) and M4 (blue) treated with 3 μg/kg (right panel). Plasma CD123-NKCE concentrations were monitored 1.5, 5, 24, 48, 72, 168, 240, 336, 504 and 672 hours (that is 0.04, 0.06, 0.21, 1, 2, 3, 7, 10, 14, 21 and 28 days) after the start of the one-hour infusion. The lower limit of quantification (LLOQ; 0.25 ng/mL) is indicated by the horizontal dotted line. **d**, Individual Anti-Drug antibody (ADA) ratio of monkeys M1 (orange) and M2 (purple) treated with 3 mg/kg, and monkeys M3 (black) and M4 (blue) treated with 3 μg/kg. Presence of ADA in plasma was monitored at predose (baseline) and at day 1, 7, 10, and 28 after the start of the one-hour infusion.



Extended Data Fig. 4 | Expression of CD64 on target cells inhibits anti-B7-H3 antibody-mediated ADCC in vitro. **a**, Comparison of the cytotoxicities of an anti-B7-H3 antibody (B7-H3-IgG1) and of an anti-B7-H3 NKCE molecule co-engaging Nkp46 and CD16a (B7-H3-NKCE). CD64⁻ A375 and LN229

cells, and CD64-positive THP-1 cells were used as the targets and purified resting NK cells as effectors. The data shown are representative of three independent experiments. **b**, Phenotype of the target cells used in **a** showing the expression of B7-H3, CD32a/b, CD64 and CD123 by flow cytometry.

Extended Data Table 1 | Monovalent affinities of CD123-NKCE binding to human and cynomolgus ligands

Human proteins	K_D (nM) \pm SD	
	CD123-NKCE	Human IgG1 control
CD123	0.40 \pm 0.02	N/A
NKp46	16.6 \pm 1.1	N/A
FcRn ^a	109 \pm 28	94 \pm 25
CD64 (FcγRI)	0.2 \pm 0.0	0.2 \pm 0.0
CD32a (FcγRIIa)	1222 \pm 99	1574 \pm 108
CD32b (FcγRIIb)	3196 \pm 375	4232 \pm 483
CD16a (FcγRIIIa /158F)	2606 \pm 91	2820 \pm 58
CD16a (FcγRIIIa /158V)	462 \pm 12	575 \pm 16
CD16b (FcγRIIIb)	6688 \pm 413	7541 \pm 838
Cynomolgus proteins		
CD123	1.23 \pm 0.13	N/A
NKp46	29.0 \pm 1.7	N/A
FcRn ^a	282 \pm 41	237 \pm 22
CD64 (FcγRI)	12 \pm 1	18 \pm 2
CD32a (FcγRIIa)	5177 \pm 290	6336 \pm 377
CD32b (FcγRIIb)	1891 \pm 130	2320 \pm 165
CD16 (FcγRIII)	466 \pm 36	580 \pm 56

^aexperiment performed at +25°C pH5.6; default condition: +25°C pH7.4. N/A: not applicable. SD: standard deviation. K_D : Dissociation constant. N=5 for CD123 and NKp46 and N=3 for all other proteins.

Extended Data Table 2 | Individual CD123-NKCE plasma concentration values of cynomolgus monkeys treated with CD123-NKCE

Day	Sampling	Concentration in plasma (ng/mL)							
		0.1 mg/kg/administration				3 mg/kg/administration			
		M1♂	M2♂	F3♀	F4♀	M5♂	M6♂	F7♀	F8♀
1	Predose	<LLOQ	<LLOQ	<LLOQ	<LLOQ	2.27	<LLOQ	<LLOQ	<LLOQ
1	1h	1,750	1,200	1,550	1,870	37,000	68,700	100,000	46,200 ^b
1	1.5h	1,100	1,520	1,390	1,750	78,600	67,000	98,600	48,300 ^b
1	5h	736	1,350	986	469	64,100	72,200	76,300	47,500 ^b
2	24h	160	381	250	448	221,000 ^a	30,800	55,200	41,500 ^b
4	72h	1.66	9.17	7.83	14.8	31,600	31,100	27,500	29,100 ^b
8	168h/Predose	<LLOQ	0.484	0.698	1.18	16,000	17,300	20,100	37,800
8	1h	1,340	3.32	1,980	1,610	92,000	91,900	137,000	87,500
8	1.5h	1,250	29.6	1,680	1,460	89,900	88,400	110,000	82,500
8	5h	892	132	1,280	1,210	38,600	72,900	74,800	88,300
9	24h	239	78.2	554	512	64,500	61,200	46,100	65,200
11	72h	1.17	35.7	43.8	20.8	46,300	47,100	23,000	30,500
15	168h/Predose	<LLOQ	<LLOQ	2.45	<LLOQ	45,000	51.8	<LLOQ	<LLOQ
15	1h	19.3	205	256	5.61	124,000	21,600	2,310	11,900
15	1.5h	5.53	105	190	3.30	75,900	33,600	497	9,800
15	5h	<LLOQ	22.2	157	<LLOQ	85,400	10,600	246	1,170
16	24h	<LLOQ	0.333	35.1	<LLOQ	51,700	300	<LLOQ	37.9
18	72h	nd	nd	nd	nd	nd	nd	nd	nd
22	168h/Predose	<LLOQ	<LLOQ	<LLOQ	<LLOQ	9,120	<LLOQ	<LLOQ	1.09
22	1h	0.998	<LLOQ	<LLOQ	<LLOQ	61,600	365	<LLOQ	149
22	1.5h	<LLOQ	<LLOQ	<LLOQ	<LLOQ	55,500	228	<LLOQ	53.7
22	5h	<LLOQ	<LLOQ	<LLOQ	<LLOQ	44,000	26.3	<LLOQ	<LLOQ
23	24h	<LLOQ	<LLOQ	<LLOQ	<LLOQ	26,100	<LLOQ	<LLOQ	<LLOQ
25	72h	nd	nd	nd	nd	nd	nd	nd	nd
29	168h	<LLOQ	<LLOQ	<LLOQ	<LLOQ	110	<LLOQ	<LLOQ	0.525 ^a

Individual CD123-NKCE plasma concentration values after a weekly repeat 1-hour intravenous infusion at 0.1 and 3 mg/kg/administration for 4 weeks (on Days 1, 8, 15 and 22) to cynomolgus monkeys are shown. Values are rounded to 3 significant figures. LLOQ (Lower Limit Of Quantification) 0.250 ng/mL; ^aaberrant value excluded for TK analysis; ^bGiven as indicative due to a technical issue during 1-hour infusion on Day 1 (that is, 50% of the dose received subcutaneously); nd: not done

Extended Data Table 3 | Individual anti-drug antibody (ADA) ratio of cynomolgus monkeys treated with CD123-NKCE

Day	Sampling	ADA ratio (change from baseline)							
		0.1 mg/kg/administration				3 mg/kg/administration			
		M1♂	M2♂	F3♀	F4♀	M5♂	M6♂	F7♀	F8♀
1	Pre-dose	1.0	1.0	1.0	1.0	1.0	1.0	1.0	1.0
8	Pre-dose	1.8	1.0	1.0	1.0	1.0	1.0	1.1	0.9
15	Pre-dose	4.5	1.2	1.1	1.9	1.1	1.7	1.6	2.2
22	Pre-dose	4.8	2.0	1.8	3.7	1.0	3.1	5.6	3.0
29	Day22+168h	5.6	2.9	3.1	4.6	1.0	3.9	5.9	6.1

Individual anti-drug antibody (ADA) ratio (fold-change from baseline value collected at Day 1 Predose) after a weekly repeat 1-hour intravenous infusion of CD123-NKCE at 0.1 and 3 mg/kg/administration for 4 weeks (on Days 1, 8, 15 and 22) to cynomolgus monkeys are shown. Under the assay conditions, the presence of ADA is considered to be significant when the ADA ratio is above 3.0 or, for ratio below 3.0, when the ratio increase with time.

Extended Data Table 4 | Individual IL-6 plasma concentration values of cynomolgus monkeys treated with CD123-NKCE

Day	Sampling	Concentration in plasma (ng/mL)							
		0.1 mg/kg/administration				3 mg/kg/administration			
		M1♂	M2♂	F3♀	F4♀	M5♂	M6♂	F7♀	F8♀
1	Predose	<LLOQ	<LLOQ	0.84	0.54	<LLOQ	<LLOQ	<LLOQ	2.09
1	1h	1.52	1.92	3.12	4.65	1.49	1.61	2.63	7.99
1	1.5h	2.99	4.54	5.09	6.79	2.17	2.98	5.61	14.37
1	5h	1.83	3.00	3.17	3.55	1.57	8.92	11.41	15.86
2	24h	<LLOQ	<LLOQ	0.66	1.98	0.79	1.96	2.15	1.61
8	168h/Predose	<LLOQ	<LLOQ	<LLOQ	<LLOQ	0.73	1.63	1.52	0.57
8	1h	1.42	2.12	5.04	2.60	1.65	2.35	2.74	4.48
8	1.5h	2.97	18.84	9.85	2.46	1.90	2.5	3.92	8.50
8	5h	2.15	18.89	7.69	1.39	1.53	38.04	2.34	2.71
9	24h	0.92	4.23	1.18	1.56	0.68	3.98	11.58	1.03
15	168h/Predose	<LLOQ	<LLOQ	<LLOQ	<LLOQ	<LLOQ	<LLOQ	0.62	1.58
15	1h	1.20	1.98	2.93	1.63	2.17	3.14	7.67	68.51
15	1.5h	1.47	1.88	5.72	1.65	2.35	5.02	12.19	85.36
15	5h	2.33	1.33	1.57	1.33	5.53	2.01	4.09	7.11
16	24h	<LLOQ	<LLOQ	1.48	6.47	2.76	<LLOQ	1.40	0.71
22	168h/Predose	<LLOQ	<LLOQ	<LLOQ	<LLOQ	1.16	<LLOQ	1.34	1.11
22	1h	2.22	2.79	1.35	4.07	3.12	123.36	27.39	150.97
22	1.5h	3.54	3.52	2.23	5.08	2.83	121.88	51.43	159.71
22	5h	2.68	4.42	2.89	22.72	2.56	4.07	6.35	22.23
23	24h	<LLOQ	1.53	<LLOQ	0.81	4.52	<LLOQ	1.10	1.29
29	168h	0.79	<LLOQ	<LLOQ	<LLOQ	<LLOQ	0.74	<LLOQ	0.69

Individual IL-6 plasma concentration values after a weekly repeat 1-hour intravenous infusion of CD123-NKCE at 0.1 and 3 mg/kg/administration for 4 weeks (on Days 1, 8, 15 and 22) to cynomolgus monkeys are shown. LLOQ (Lower Limit Of Quantification): 0.53 pg/mL.

Extended Data Table 5 | Individual absolute counts of basophils and total CD123-positive cells in blood and bone marrow of cynomolgus monkeys treated with CD123-NKCE

Day	Sampling	0.1 mg/kg/administration				3 mg/kg/administration			
		M1♂	M2♂	F3♀	F4♀	M5♂	M6♂	F7♀	F8♀
Absolute count of CD123-positive basophils in blood (cells/ μ L)									
	Predose	1.16	2.79	8.60	2.25	5.65	11.6	15.1	<DL
1	1.5h	<DL	<DL	<DL	<DL	<DL	<DL	<DL	<DL
1	5h	<DL	<DL	<DL	<DL	<DL	<DL	<DL	<DL
2		<DL	<DL	<DL	<DL	<DL	<DL	<DL	<DL
4		<DL	<DL	<DL	<DL	<DL	<DL	<DL	<DL
9		<DL	<DL	<DL	<DL	<DL	<DL	<DL	<DL
15	1.5h	<DL	<DL	<DL	<DL	<DL	<DL	<DL	<DL
16		1.90	<DL	<DL	<DL	<DL	<DL	1.87	<DL
23		1.56	<DL	<DL	7.61	<DL	10.4	34.7	9.58
29		11.8	3.30	<DL	34.5	<DL	24.9	62.3	17.0
50		4.19	nd	6.30	nd	13.1	nd	12.9	nd
Absolute count of total CD123-positive cells in blood (cells/ μ L)									
	Predose	6.26	6.32	21.9	4.02	9.72	22.8	19.3	1.59
1	1.5h	5.90	1.83	3.01	3.74	1.50	<DL	1.18	1.24
1	5h	4.06	1.40	<DL	1.90	<DL	<DL	<DL	<DL
2		3.79	2.00	<DL	2.47	<DL	2.08	2.30	1.48
4		10.3	1.95	2.47	2.43	1.54	1.32	1.84	2.80
9		1.44	<DL	<DL	<DL	<DL	<DL	<DL	<DL
15	1.5h	5.77	2.16	2.40	3.25	1.15	8.14	12.9	12.3
16		17.7	3.77	2.97	6.42	1.43	7.16	10.2	8.91
23		18.5	8.33	9.52	12.2	1.28	58.5	49.7	32.4
29		33.9	18.2	29.5	47.0	4.15	82.9	72.1	38.1
50		8.81	nd	14.5	nd	16.8	nd	17.3	nd
Absolute count of CD123-positive basophils in bone marrow (cells/ μ L)									
	Predose	439	11.5	30.2	30.0	21.4	14.7	155	21.3
9		<DL	<DL	<DL	<DL	<DL	<DL	<DL	<DL
29		74.5	25.6	50.2	89.2	<DL	50.0	235.6	131
50		54.0	nd	185	nd	29.6	nd	43.9	nd
Absolute count of total CD123-positive cells in bone marrow (cells/ μ L)									
	Predose	914	19.8	45.9	51.1	61.6	28.9	218	41.6
9		5.85	<DL	<DL	<DL	<DL	<DL	<DL	<DL
29		140	49.6	192	142	68.4	98.1	311	200.8
50		112	nd	402	nd	50.9	nd	71.6	nd

Individual absolute counts of basophils and total CD123-positive cells in blood and bone marrow after a weekly repeat 1-hour intravenous infusion of CD123-NKCE at 0.1 and 3 mg/kg/ administration for 4 weeks to cynomolgus monkeys are shown. DL (detection limit): 1.15 cells/ μ L (blood) or 2.10 cells/ μ L (bone marrow); nd: not done.

Reporting Summary

Nature Portfolio wishes to improve the reproducibility of the work that we publish. This form provides structure for consistency and transparency in reporting. For further information on Nature Portfolio policies, see our [Editorial Policies](#) and the [Editorial Policy Checklist](#).

Statistics

For all statistical analyses, confirm that the following items are present in the figure legend, table legend, main text, or Methods section.

n/a Confirmed

- The exact sample size (n) for each experimental group/condition, given as a discrete number and unit of measurement
- A statement on whether measurements were taken from distinct samples or whether the same sample was measured repeatedly
- The statistical test(s) used AND whether they are one- or two-sided
Only common tests should be described solely by name; describe more complex techniques in the Methods section.
- A description of all covariates tested
- A description of any assumptions or corrections, such as tests of normality and adjustment for multiple comparisons
- A full description of the statistical parameters including central tendency (e.g. means) or other basic estimates (e.g. regression coefficient) AND variation (e.g. standard deviation) or associated estimates of uncertainty (e.g. confidence intervals)
- For null hypothesis testing, the test statistic (e.g. F , t , r) with confidence intervals, effect sizes, degrees of freedom and P value noted
Give P values as exact values whenever suitable.
- For Bayesian analysis, information on the choice of priors and Markov chain Monte Carlo settings
- For hierarchical and complex designs, identification of the appropriate level for tests and full reporting of outcomes
- Estimates of effect sizes (e.g. Cohen's d , Pearson's r), indicating how they were calculated

Our web collection on [statistics for biologists](#) contains articles on many of the points above.

Software and code

Policy information about [availability of computer code](#)

Data collection

Meso Quickplex SQ 120 system and MSD Workbench 3.0.18 software : MesoScale Discovery (used to measure cytokines concentrations)
 Cellometer Auto T4 plus cell counter: Nexcelom Bioscience (used to count cells)
 TopCount NXT™ (Microplate Scintillation and Luminescence Counter): Perkin Elmer (used to detect radioactivity)
 FACS CANTO II n²: BD Bioscience(used to read fluorescence)
 BD LSR Fortessa™ X-20 n²: BD Bioscience (used to detect fluorescence)
 Biacore T200 apparatus :Biacore GE Healthcare & Cytiva, Uppsala (Catalog No. 28975001)(used to acquire affinity data)
 BD FACSDiva v8.0 software (for flow cytometry data acquisition)
 MACSQuant® Analyzer from Miltenyi Biotec (used to read fluorescence)

Data analysis

VenturiOne® v6.1 software (Applied Cytometry Inc.) (for flow cytometry analysis)
 FlowJo v10.5.2 software (for flow cytometry data analysis)
 Kaluza analysis v1.3 (for flow cytometry data analysis)
 GraphPad Prism v8.0.2 and v8.3.0 (for graphics and statistical analysis)
 GraphPad Prism v8.3.0 (for graphics and statistical analysis of in vivo data)
 Biacore T200 Evaluation software v3.0 and v3.1 (to analyze affinity data)
 Phoenix v1.4 (including WinNonLin v 6.4) Pharsight (Certara Inc.) (for PK and TK analysis)
 Excel 2019 (for MSD analysis)

For manuscripts utilizing custom algorithms or software that are central to the research but not yet described in published literature, software must be made available to editors and reviewers. We strongly encourage code deposition in a community repository (e.g. GitHub). See the Nature Portfolio [guidelines for submitting code & software](#) for further information.

Data

Policy information about [availability of data](#)

All manuscripts must include a [data availability statement](#). This statement should provide the following information, where applicable:

- Accession codes, unique identifiers, or web links for publicly available datasets
- A description of any restrictions on data availability
- For clinical datasets or third party data, please ensure that the statement adheres to our [policy](#)

All data supporting the results are available in the main text or the supplementary materials. The detailed molecular organization and the sequences of the NKCE used in the present study can be found in Supplementary Information Figure 1 and Figure 2, and in patent WO2016207273 and WO2022144836A1. Recombinant proteins were built from sequences found at <https://www.ncbi.nlm.nih.gov>.

Human research participants

Policy information about [studies involving human research participants and Sex and Gender in Research](#).

Reporting on sex and gender	N/A
Population characteristics	N/A
Recruitment	N/A
Ethics oversight	N/A

Note that full information on the approval of the study protocol must also be provided in the manuscript.

Field-specific reporting

Please select the one below that is the best fit for your research. If you are not sure, read the appropriate sections before making your selection.

Life sciences Behavioural & social sciences Ecological, evolutionary & environmental sciences

For a reference copy of the document with all sections, see [nature.com/documents/nr-reporting-summary-flat.pdf](https://www.nature.com/documents/nr-reporting-summary-flat.pdf)

Life sciences study design

All studies must disclose on these points even when the disclosure is negative.

Sample size	For in vivo studies (mouse model), the sample size was set to a minimum of 10 mice per groups to ensure a proper statistical analysis of data. <input checked="" type="checkbox"/> Sample size determination was not applicable to any other studies than in vivo studies.
Data exclusions	Data were excluded when technical issues or aberrant values were identified. Excluded values are specified in the manuscript tables
Replication	Experiments were performed on a minimum of 3 (and up to 10) individual healthy donor or patient samples to validate reproducibility of findings. For in vivo experiments, the dose-efficacy studies were repeated two to four times (pooled data are represented). All replications were successful with good consistency between healthy donors, patient samples and attempts.
Randomization	N/A. None of the experimental methods used in this study necessitated any randomization of sample groups.
Blinding	N/A. None of the experimental methods used in this study necessitated any blinding.

Behavioural & social sciences study design

All studies must disclose on these points even when the disclosure is negative.

Study description	Briefly describe the study type including whether data are quantitative, qualitative, or mixed-methods (e.g. qualitative cross-sectional, quantitative experimental, mixed-methods case study).
Research sample	State the research sample (e.g. Harvard university undergraduates, villagers in rural India) and provide relevant demographic information (e.g. age, sex) and indicate whether the sample is representative. Provide a rationale for the study sample chosen. For studies involving existing datasets, please describe the dataset and source.

Sampling strategy	<i>Describe the sampling procedure (e.g. random, snowball, stratified, convenience). Describe the statistical methods that were used to predetermine sample size OR if no sample-size calculation was performed, describe how sample sizes were chosen and provide a rationale for why these sample sizes are sufficient. For qualitative data, please indicate whether data saturation was considered, and what criteria were used to decide that no further sampling was needed.</i>
Data collection	<i>Provide details about the data collection procedure, including the instruments or devices used to record the data (e.g. pen and paper, computer, eye tracker, video or audio equipment) whether anyone was present besides the participant(s) and the researcher, and whether the researcher was blind to experimental condition and/or the study hypothesis during data collection.</i>
Timing	<i>Indicate the start and stop dates of data collection. If there is a gap between collection periods, state the dates for each sample cohort.</i>
Data exclusions	<i>If no data were excluded from the analyses, state so OR if data were excluded, provide the exact number of exclusions and the rationale behind them, indicating whether exclusion criteria were pre-established.</i>
Non-participation	<i>State how many participants dropped out/declined participation and the reason(s) given OR provide response rate OR state that no participants dropped out/declined participation.</i>
Randomization	<i>If participants were not allocated into experimental groups, state so OR describe how participants were allocated to groups, and if allocation was not random, describe how covariates were controlled.</i>

Ecological, evolutionary & environmental sciences study design

All studies must disclose on these points even when the disclosure is negative.

Study description	<i>Briefly describe the study. For quantitative data include treatment factors and interactions, design structure (e.g. factorial, nested, hierarchical), nature and number of experimental units and replicates.</i>
Research sample	<i>Describe the research sample (e.g. a group of tagged <i>Passer domesticus</i>, all <i>Stenocereus thurberi</i> within Organ Pipe Cactus National Monument), and provide a rationale for the sample choice. When relevant, describe the organism taxa, source, sex, age range and any manipulations. State what population the sample is meant to represent when applicable. For studies involving existing datasets, describe the data and its source.</i>
Sampling strategy	<i>Note the sampling procedure. Describe the statistical methods that were used to predetermine sample size OR if no sample-size calculation was performed, describe how sample sizes were chosen and provide a rationale for why these sample sizes are sufficient.</i>
Data collection	<i>Describe the data collection procedure, including who recorded the data and how.</i>
Timing and spatial scale	<i>Indicate the start and stop dates of data collection, noting the frequency and periodicity of sampling and providing a rationale for these choices. If there is a gap between collection periods, state the dates for each sample cohort. Specify the spatial scale from which the data are taken</i>
Data exclusions	<i>If no data were excluded from the analyses, state so OR if data were excluded, describe the exclusions and the rationale behind them, indicating whether exclusion criteria were pre-established.</i>
Reproducibility	<i>Describe the measures taken to verify the reproducibility of experimental findings. For each experiment, note whether any attempts to repeat the experiment failed OR state that all attempts to repeat the experiment were successful.</i>
Randomization	<i>Describe how samples/organisms/participants were allocated into groups. If allocation was not random, describe how covariates were controlled. If this is not relevant to your study, explain why.</i>
Blinding	<i>Describe the extent of blinding used during data acquisition and analysis. If blinding was not possible, describe why OR explain why blinding was not relevant to your study.</i>

Did the study involve field work? Yes No

Field work, collection and transport

Field conditions	<i>Describe the study conditions for field work, providing relevant parameters (e.g. temperature, rainfall).</i>
Location	<i>State the location of the sampling or experiment, providing relevant parameters (e.g. latitude and longitude, elevation, water depth).</i>
Access & import/export	<i>Describe the efforts you have made to access habitats and to collect and import/export your samples in a responsible manner and in compliance with local, national and international laws, noting any permits that were obtained (give the name of the issuing authority, the date of issue, and any identifying information).</i>

Reporting for specific materials, systems and methods

We require information from authors about some types of materials, experimental systems and methods used in many studies. Here, indicate whether each material, system or method listed is relevant to your study. If you are not sure if a list item applies to your research, read the appropriate section before selecting a response.

Materials & experimental systems

- | n/a | Involved in the study |
|-------------------------------------|---|
| <input type="checkbox"/> | <input checked="" type="checkbox"/> Antibodies |
| <input type="checkbox"/> | <input checked="" type="checkbox"/> Eukaryotic cell lines |
| <input checked="" type="checkbox"/> | <input type="checkbox"/> Palaeontology and archaeology |
| <input type="checkbox"/> | <input checked="" type="checkbox"/> Animals and other organisms |
| <input checked="" type="checkbox"/> | <input type="checkbox"/> Clinical data |
| <input checked="" type="checkbox"/> | <input type="checkbox"/> Dual use research of concern |

Methods

- | n/a | Involved in the study |
|-------------------------------------|--|
| <input checked="" type="checkbox"/> | <input type="checkbox"/> ChIP-seq |
| <input type="checkbox"/> | <input checked="" type="checkbox"/> Flow cytometry |
| <input checked="" type="checkbox"/> | <input type="checkbox"/> MRI-based neuroimaging |

Antibodies

Antibodies used

Human NK cell activation panel CD107a/b-APC cocktail (Anti-CD56-PE-Vio770/Anti-CD107a-APC/Anti-CD107b-APC/Anti-CD3-VioBlue)/Miltenyi/130-095-212 (dilution: 1/10)
 Anti-CD56-PEVio770/Miltenyi/130-100-676 (dilution: 1/50)
 Anti-Nkp46-PE/Beckman Coulter /IM3711 (dilution: 1/50)
 Anti-CD16-PE/BD Biosciences/556619 (dilution: 1/20)
 Anti-CD16-APC-Cy7/BD Biosciences/557758 (dilution: 1/20)
 Anti-CD32-PE/Beckman Coulter/IM1935 (dilution: 1/10)
 Anti-CD64-PE/Beckman Coulter/IM3601U (dilution: 1/10)
 Anti-CD64-PerCp-Cy5.5/BD Biosciences/561194 (dilution: 1/20)
 Anti-CD123-PE/Biolegend/306006 (dilution: 1/20)
 Anti-CD123-APC/Biolegend/396706 (dilution: 1/20)
 Anti-CD69-FITC/Miltenyi/130-113-523 (dilution: 1/200)
 Anti-CD45-APC/Miltenyi/130-110-771 (dilution: 1/50)
 Anti-CD33-BB515/BD Biosciences/564588 (dilution: 1/40)
 Anti-CD3-BV510/BD Biosciences/740187 (dilution: 1/40)
 Anti-CD56-PECy7/BD Biosciences/557747 (dilution: 1/40)
 Anti-CD107a-APC/Miltenyi/130-095-510 (dilution: 1/10)
 Anti-CD107b-APC/Miltenyi/130-103-960 (dilution: 1/10)
 Anti-CD107a-PE/Miltenyi/130-111-621 (dilution: 1/50)
 Anti-CD107b-PE/Miltenyi/130-118-818 (dilution: 1/50)
 Anti-TNF-BUV395/BD Biosciences/563996 (dilution: 1/40)
 Anti-IFN γ -BV605/Biolegend/502536 (dilution: 1/40)
 Anti-human MIP1 β -PE/BD Biosciences/550078 (dilution: 1/40)
 Anti-CD3-Pacific Blue/BD Biosciences/624033 (dilution: 1/50)
 IgE-VioBlue/Miltenyi Biotec/130-117-931 (dilution : 1/50)
 Anti-CD45-BV510 (cynomolgus)/BD Biosciences/563530 (dilution: 1/20)
 Anti-CD14-FITC (cynomolgus)/Miltenyi Biotec/130-110-518 (dilution: 1/50)
 Anti-CD123-PE (cynomolgus)/BD Biosciences/554529 (dilution : 1/20)
 Anti-CD33-PE Vio770 (cynomolgus)/Miltenyi Biotec/130-113-350 (dilution : 1/50)
 Anti-CD193-APC (cynomolgus)/Biolegend/310708 (dilution: 1/20)
 Anti-CD203c-APC (cynomolgus)/Invitrogen/17-2039-42 (dilution: 1/20)
 Anti-CD14-VioBlue/Miltenyi Biotec/130-110-524 (dilution: 1/35)
 IgE-APC/Miltenyi Biotec/130-117-930 (dilution: 1/35)
 Anti- ϵ / δ TCR-APC-Vio770/Miltenyi Biotec/130-113-536 (dilution: 1/20)
 REA-control-VioBlue/Miltenyi Biotec/130-104-609 (dilution: 1/12)
 REA-control-APC/Miltenyi Biotec/130-104-614 (dilution: 1/12)
 REA-control-APC Vio770 /Miltenyi Biotec/130-104-618 (dilution: 1/12)
 Polyclonal Anti-asialo-GM1/Biolegend/Poly21460

Validation

For flow cytometry studies, primary antibodies targeting NHP antigens were titrated using cynomolgus PBMCs under the same conditions as those used in the study. Primary antibodies targeting human antigens were titrated using human PBMCs, or human purified NK cells or human AML cell lines according to their use in the corresponding studies and under the same conditions as those used in the studies.

Eukaryotic cell lines

Policy information about [cell lines and Sex and Gender in Research](#)

Cell line source(s)	KG-1a, Kasumi-6, GDM-1, MOLM-13 and THP-1 AML cell lines were purchased at ATCC. M-07e, EOL-1, Kasumi-1, F36-P, NB-4, OCI-AML2, MV4-11, OCI-AML3, and SKM-1 AML cell lines were purchased at DSMZ.
Authentication	None of the cell lines used were authenticated
Mycoplasma contamination	All cell lines were tested negative for mycoplasma
Commonly misidentified lines (See ICLAC register)	N/A. No commonly misidentified lines were used in the study.

Palaeontology and Archaeology

Specimen provenance	<i>Provide provenance information for specimens and describe permits that were obtained for the work (including the name of the issuing authority, the date of issue, and any identifying information). Permits should encompass collection and, where applicable, export.</i>
Specimen deposition	<i>Indicate where the specimens have been deposited to permit free access by other researchers.</i>
Dating methods	<i>If new dates are provided, describe how they were obtained (e.g. collection, storage, sample pretreatment and measurement), where they were obtained (i.e. lab name), the calibration program and the protocol for quality assurance OR state that no new dates are provided.</i>
<input type="checkbox"/> Tick this box to confirm that the raw and calibrated dates are available in the paper or in Supplementary Information.	
Ethics oversight	<i>Identify the organization(s) that approved or provided guidance on the study protocol, OR state that no ethical approval or guidance was required and explain why not.</i>

Note that full information on the approval of the study protocol must also be provided in the manuscript.

Animals and other research organisms

Policy information about [studies involving animals](#); [ARRIVE guidelines](#) recommended for reporting animal research, and [Sex and Gender in Research](#)

Laboratory animals	Mus musculus /NOD.Cg-Prkdcscid/J ; commonly referred to as SCID For in vivo efficacy study, mice were 13 to 15 weeks-old and weighed from 17.8 to 24.9 grams at the start of the study. For comparative study in the absence of presence of NK cell, mice were 10 to 12 weeks-old and weighed from 16.5 to 24.4 grams at the start of the study. They were housed on a 12 hours light/dark cycle. Environmental conditions including animal maintenance, room temperature (22°C ± 2°C), relative humidity (55% ± 15%) and lighting times were recorded by the supervisor of laboratory animal sciences and welfare and the records were archived. Macaca fascicularis (Mauritius) / Cynomolgus non-human primates / males and females were used for the study.
Wild animals	N/A. No wild animals were used in this study
Reporting on sex	For repeated dosing in non human primate, sex were considered in the study design and an equal number of females (4 animals) and males (4 animals) were included in the study. Data are reported desegregated for each animal. All the findings presented in the study apply for both sex.
Field-collected samples	N/A. No samples were collected in fields
Ethics oversight	All animal procedures were approved by the Sanofi Animal Care and Use Committee, followed the French and European regulations on care and protection of the Laboratory Animals, and in accordance with the standards of the Association for Assessment and Accreditation of Laboratory Animal Care (AAALAC).

Note that full information on the approval of the study protocol must also be provided in the manuscript.

Clinical data

Policy information about [clinical studies](#)

All manuscripts should comply with the ICMJE [guidelines for publication of clinical research](#) and a completed [CONSORT checklist](#) must be included with all submissions.

Clinical trial registration	<i>Provide the trial registration number from ClinicalTrials.gov or an equivalent agency.</i>
Study protocol	<i>Note where the full trial protocol can be accessed OR if not available, explain why.</i>

Data collection

Describe the settings and locales of data collection, noting the time periods of recruitment and data collection.

Outcomes

Describe how you pre-defined primary and secondary outcome measures and how you assessed these measures.

Dual use research of concern

Policy information about [dual use research of concern](#)

Hazards

Could the accidental, deliberate or reckless misuse of agents or technologies generated in the work, or the application of information presented in the manuscript, pose a threat to:

No | Yes

- Public health
- National security
- Crops and/or livestock
- Ecosystems
- Any other significant area

Experiments of concern

Does the work involve any of these experiments of concern:

No | Yes

- Demonstrate how to render a vaccine ineffective
- Confer resistance to therapeutically useful antibiotics or antiviral agents
- Enhance the virulence of a pathogen or render a nonpathogen virulent
- Increase transmissibility of a pathogen
- Alter the host range of a pathogen
- Enable evasion of diagnostic/detection modalities
- Enable the weaponization of a biological agent or toxin
- Any other potentially harmful combination of experiments and agents

ChIP-seq

Data deposition

- Confirm that both raw and final processed data have been deposited in a public database such as [GEO](#).
- Confirm that you have deposited or provided access to graph files (e.g. BED files) for the called peaks.

Data access links

*May remain private before publication.**For "Initial submission" or "Revised version" documents, provide reviewer access links. For your "Final submission" document, provide a link to the deposited data.*

Files in database submission

Provide a list of all files available in the database submission.

Genome browser session

*(e.g. [UCSC](#))**Provide a link to an anonymized genome browser session for "Initial submission" and "Revised version" documents only, to enable peer review. Write "no longer applicable" for "Final submission" documents.*

Methodology

Replicates

Describe the experimental replicates, specifying number, type and replicate agreement.

Sequencing depth

Describe the sequencing depth for each experiment, providing the total number of reads, uniquely mapped reads, length of reads and whether they were paired- or single-end.

Antibodies

Describe the antibodies used for the ChIP-seq experiments; as applicable, provide supplier name, catalog number, clone name, and lot number.

Peak calling parameters

Specify the command line program and parameters used for read mapping and peak calling, including the ChIP, control and index files used.

Data quality

Describe the methods used to ensure data quality in full detail, including how many peaks are at FDR 5% and above 5-fold enrichment.

Software

Describe the software used to collect and analyze the ChIP-seq data. For custom code that has been deposited into a community repository, provide accession details.

Flow Cytometry

Plots

Confirm that:

- The axis labels state the marker and fluorochrome used (e.g. CD4-FITC).
- The axis scales are clearly visible. Include numbers along axes only for bottom left plot of group (a 'group' is an analysis of identical markers).
- All plots are contour plots with outliers or pseudocolor plots.
- A numerical value for number of cells or percentage (with statistics) is provided.

Methodology

Sample preparation

Healthy human buffy coats were provided by the Etablissement Français du Sang (EFS, the French blood service, Marseille; (AC-2019-3428)). Peripheral mononuclear cells (PBMC) were isolated from buffy coats by Ficoll density gradient centrifugation. Human NK cell were purified from PBMC with a bead-based negative selection kit from STEMCELL Technologies or Miltenyi Biotec.
For non-human primate studies, whole blood (100µl) and bone marrow (50µl) were lysed before to be stained with the dedicated antibody cocktails. After 10mn at ambient temperature, the samples were washed, centrifuged, and fixed before acquisition.

Instrument

FACS CANTO II n°2: BD Bioscience(used to read fluorescence)
BD LSR Fortessa™ X-20 n°2: BD Bioscience (used to detect fluorescence)
MACSQuant® Analyzer from Miltenyi Biotec (used to read fluorescence)

Software

VenturiOne® v6.1 software (Applied Cytometry Inc.) (for flow cytometry analysis)
FlowJo v10.5.2 software (for flow cytometry data analysis)
BD FACSDiva v8.0 software (for flow cytometry data acquisition)
Kaluza analysis v1.3 (for flow cytometry data analysis)

Cell population abundance

For in vitro experiments, human NK cells were purified from PBMCs by negative selection with kits from Miltenyi Biotec, with a mean of purity of about 90%. Only samples with NK cell purity superior to 80% were kept for the study.

Gating strategy

NK cells: Time Gate / Single cells (SSC-A SSC-W) / Living cells (livedead negative) / Leucocytes (CD45+)/ CD3- / CD56+
Human Basophils : Time Gate / Single cells (SSC-A FSC-A) / Living cells (livedead negative) / CD14- / IgE+ (i.e. FcepsilonRI+) / TCRalpha -
Non human primate Basophils : Single cells (SSC-A FSC-A) / viable cells (Zombie NIR negative) / CD45+ / CD193+/CD203c+ / IgE+ (i.e. FcepsilonRI+)
AML blasts: Time Gate / Single cells (SSC-A SSC-W) / Living cells (livedead neg) / Leucocytes (CD45+)/ CD33+

- Tick this box to confirm that a figure exemplifying the gating strategy is provided in the Supplementary Information.

Magnetic resonance imaging

Experimental design

Design type

Indicate task or resting state; event-related or block design.

Design specifications

Specify the number of blocks, trials or experimental units per session and/or subject, and specify the length of each trial or block (if trials are blocked) and interval between trials.

Behavioral performance measures

State number and/or type of variables recorded (e.g. correct button press, response time) and what statistics were used to establish that the subjects were performing the task as expected (e.g. mean, range, and/or standard deviation across subjects).

Acquisition

Imaging type(s)

Specify: functional, structural, diffusion, perfusion.

Field strength

Specify in Tesla

Sequence & imaging parameters

Specify the pulse sequence type (gradient echo, spin echo, etc.), imaging type (EPI, spiral, etc.), field of view, matrix size, slice thickness, orientation and TE/TR/flip angle.

Area of acquisition

State whether a whole brain scan was used OR define the area of acquisition, describing how the region was determined.

Diffusion MRI Used Not used

Preprocessing

Preprocessing software	<i>Provide detail on software version and revision number and on specific parameters (model/functions, brain extraction, segmentation, smoothing kernel size, etc.).</i>
Normalization	<i>If data were normalized/standardized, describe the approach(es): specify linear or non-linear and define image types used for transformation OR indicate that data were not normalized and explain rationale for lack of normalization.</i>
Normalization template	<i>Describe the template used for normalization/transformation, specifying subject space or group standardized space (e.g. original Talairach, MNI305, ICBM152) OR indicate that the data were not normalized.</i>
Noise and artifact removal	<i>Describe your procedure(s) for artifact and structured noise removal, specifying motion parameters, tissue signals and physiological signals (heart rate, respiration).</i>
Volume censoring	<i>Define your software and/or method and criteria for volume censoring, and state the extent of such censoring.</i>

Statistical modeling & inference

Model type and settings	<i>Specify type (mass univariate, multivariate, RSA, predictive, etc.) and describe essential details of the model at the first and second levels (e.g. fixed, random or mixed effects; drift or auto-correlation).</i>
Effect(s) tested	<i>Define precise effect in terms of the task or stimulus conditions instead of psychological concepts and indicate whether ANOVA or factorial designs were used.</i>
Specify type of analysis:	<input type="checkbox"/> Whole brain <input type="checkbox"/> ROI-based <input type="checkbox"/> Both
Statistic type for inference (See Eklund et al. 2016)	<i>Specify voxel-wise or cluster-wise and report all relevant parameters for cluster-wise methods.</i>
Correction	<i>Describe the type of correction and how it is obtained for multiple comparisons (e.g. FWE, FDR, permutation or Monte Carlo).</i>

Models & analysis

n/a | Involved in the study

- Functional and/or effective connectivity
- Graph analysis
- Multivariate modeling or predictive analysis

Functional and/or effective connectivity	<i>Report the measures of dependence used and the model details (e.g. Pearson correlation, partial correlation, mutual information).</i>
Graph analysis	<i>Report the dependent variable and connectivity measure, specifying weighted graph or binarized graph, subject- or group-level, and the global and/or node summaries used (e.g. clustering coefficient, efficiency, etc.).</i>
Multivariate modeling and predictive analysis	<i>Specify independent variables, features extraction and dimension reduction, model, training and evaluation metrics.</i>